Potassium transporter OsHAK18 mediates shoot-to-root circulation of potassium and sodium and source-to-sink translocation of soluble sugar in rice

Lirun Peng[1,2], Huojun Xiao[1,2], Ran Li[1,2], Yang Zeng[1,2], Mian Gu[1,2], Nava Moran[3], Ling Yu[1,2] *, Guohua Xu[1,2] *

Affiliation of all authors:

[1] National Key Laboratory of Crop Genetics & Germplasm Enhancement and Utilization, [2] Key Laboratory of Plant Nutrition and Fertilization in Low-Middle Reaches of the Yangtze River, Ministry of Agriculture, Nanjing Agricultural University, 210095, China. [3] The Robert H. Smith Institute of Plant Sciences and Genetics in Agriculture, The Robert H. Smith Faculty of Agriculture, Food and Environment, The Hebrew University of Jerusalem, Rehovot 76100, Israel.

***Corresponding authors.** Email: lyu@njau.edu.cn; ghxu@njau.edu.cn

ORCIDs of authors:

0000-0001-9520-3406 (L.P.); 0000-0002-2202-0729 (M.G.); 0000-0003-0831-7400 (N.M.); 0000-0001-6241-2228 (L.Y.); 0000-0002-3283-2392 (G.X.).

Running title: Transporter for shoot-to-root cycle of K and Na

One sentence summary:

Rice potassium transporter OsHAK18 mediates shoot-to-root circulation of potassium and sodium and source-to-sink translocation of soluble sugar for improving potassium use efficiency and grain yield.

Text length:

ABSTRCT: 206; Total words 7239 excluding references and legends of figures/tables.

Main figures: 8. Supplemental data: 6 figures and 6 tables.

Abstract

High-affinity potassium (K^+) transporters HAK/KUP/KT have been identified in all genome-sequenced terrestrial plants. They play important role in K^+ acquisition, translocation and enhancing salt tolerance. Here we report that the plasma-membrane-located OsHAK18 functions in K^+ and sodium (Na^+) circulation and sugar translocation in rice. OsHAK18 is expressed mainly though not exclusively in vascular tissues and in the phloem in particular. Knockout (KO) of *OsHAK18* reduced K^+ concentration in phloem sap and in the root but increased K^+ accumulation in the shoot of both Nipponbare and Zhonghua11 cultivars, while overexpression (OX) of *OsHAK18* driven by its endogenous promoter increased K^+ concentration in phloem sap and in roots, and promoted Na^+ retrieval from shoot to root under salt stress. Split-root experimental analysis for rubidium (Rb^+) uptake and circulation indicated that *OsHAK18*-OX promoted Rb^+ translocation from shoot to root. In addition, *OsHAK18*-KO increased while *OsHAK18*-OX reduced soluble sugar content in shoot while exerting opposite effects on the sugar concentration in the phloem and its content in the root. Moreover, *OsHAK18*-OX increased dramatically grain yield and K^+ physiological utilization efficiency. Taken together, our results suggest that – unlike other OsHAKs analyzed heretofore – OsHAK18 is critical to K^+ and Na^+ circulation from shoot to root and enhances the source-to-sink translocation of photo-assimilates.

Keywords: Rice; HAK transporter; Potassium and sodium circulation; soluble sugar translocation

INTRODUCTION

Potassium (K^+) is the most abundant cation in plants and is critical in maintaining ion balance, regulating turgor pressure and enzymes activity, as well as in promoting the mobilization of other nutrients and sugar (Anschutz et al., 2014; Li et al., 2018). K^+ is a highly mobile cation, it circulates in plant constituting a charge balance for anion flux, regulates photosynthetic carbon translocation from source to sink. About 40-90% of root-acquired K^+ is circulated from shoot to roots (Lu et al., 2005; Peuke et al., 2011). Such circulation may be an important feedback signal regulating root K^+ uptake and smoothing out the fluctuations of external K^+ supply (Marchner, 1996). K^+ and sodium (Na^+) ions share great similarity in physical and chemical characteristics, thus, enhancing K^+ absorption can impair Na^+ accumulation which is one of the key strategies for salt stress tolerance in glycophytes (Maathuis and Amtmann, 1999; Munns and Tester, 2008; Shabala and Cuin, 2008).

The vascular system of higher plants connects all organs together and carries out long-distance delivery of materials by two parallel structures, xylem and phloem. Xylem conducts water and solutes from root to shoot, while phloem transports mainly photo-assimilates and amino nitrogen (N) compounds in addition to water and minerals from source to sink (White and Ding, 2022). K^+ is the most abundant cation in the sap of xylem or phloem. It is absorbed by roots from soil and circulated within the plant by multiple families of K^+ channels and transporters. The Shaker family of voltage gated K^+ channels and high-affinity K^+ transporters (HAK/KUP/KTs) are major proteins underlying intercellular K^+ transport. K^+ entry into roots when the external K^+ concentration at the root surface is high occurs via the K^+ channel AKT1 down the K^+ electrochemical potential, while at a low external K^+ concentration a high-affinity K^+ uptake occurs via HAK/KUP/KT family members such as via AtHAK5 in Arabidopsis (Rubio et al., 2010) and OsHAK1 and OsHAK5 in rice (Yang et al., 2014; Chen et al., 2015). At root endoderm, the hydrophobic Casparian strip prevents apoplastic movement of K^+ into xylem sap, therefore, K^+ must enter the symplast of the endodermis and then be released into xylem sap. Protoplasts of stellar cells (xylem-enwrapping parenchyma cells) possess voltage-gated Shaker-like K^+ outwardly rectifying channels (SKOR) (Wegner and Raschke, 1994; Roberts and

Tester, 1995). These SKOR channels subserve K^+ release into the xylem sap toward the shoots (Gaymard et al., 1998). Moreover, high-affinity K^+ transporters like AtKUP7 and OsHAK5 which are also expressed in stellar cells, contribute significantly to the root-to-shoot K^+ translocation via xylem, particularly when K^+ supply is low (Yang et al., 2014; Han et al., 2016).

Phloem is comprised of longitudinally aligned sieve elements (SEs) and adjoining companion cells (CCs). It is divided into three functional domains, collection phloem, transport phloem and unloading phloem (De Schepper et al., 2013). Loading photo-assimilates and inorganic ions, mainly sucrose, into SE/CC complexes of the collection phloem at source leaves and releasing them from the unloading phloem in sink organs generate an osmotically derived hydrostatic pressure gradient (Robert, 2010). This hydrostatic pressure gradient is considered to be the major driving force for the phloem bulk flow in herbaceous plants (Crafts and Crisp, 1972; Knoblauch and Peters, 2016). High K^+ concentration in sieve tubes of phloem and a steep transmembrane pH gradient are required for sucrose/H^+ co-transporter (SUT1) to load apoplasmic sucrose into the sieve tubes at source leaves (Ayre, 2011; Julius et al., 2017). Elevation of K^+ concentration at the source as the main osmoticum which compensates for decreased loading of sucrose due to impaired SUT1 can preserve the bulk flow in phloem (Babst et al., 2022).

The transport phloem connecting the collection phloem and the unloading phloem allows a “leak out” of solutes which partially nourish the tissues in the plant axis (van Bel, 2003), or are reloaded back into the tube (Pate and Jeschke, 1995; Marschner et al., 1996). The leakage of K^+ from the companion cells of the transport phloem is conducted by the AKT2 channel of the Shaker family (Deeken et al., 2002) shown, by genetic manipulation and computational modeling, to function here as a K^+-release channel (Gajdanowicz et al., 2010). The switch of the AKT2 gating from voltage-rectifying to non-rectifying, which allows K^+ release, occurs by channel phosphorylation (Michard et al., 2005).

Solutes including K^+ are loaded into the collecting phloem via both symplastic and apoplastic routes. In the symplastic route, plasmodesmata from mesophyll cells allow the

passage of solutes directly into the companion cells, while transporters are required in the apoplastic route. Whether K^+ loading into the collecting phloem involves a K^+ channel is uncertain, though a phloem-expressed K^+ channel in maize (KZM1) can mediate K^+ influx current in *Xenopus* oocytes (Philippar et al., 2003). Patch clamp recording on mesophyll protoplast of Arabidopsis at a nearly physiological level of 10 mM K^+ revealed that all recorded cells showed outward-rectifying K^+ current but no inward K^+ current was recorded (Romano et al., 1998). This result suggests that energy-dependent K^+ transporter(s) may operate in K^+ uptake into mesophyll cells. In line with this, computational modeling also demonstrated that energy-dependent K^+ transport is required for K^+ loading into phloem in source leaves (Turgeon and Ayre, 2005). However, the identity of K^+ transporter(s) involved in phloem K circulation in plants is not known.

In this study, we provide molecular, physiological and genetic evidence that OsHAK18, a member of cluster III of HAK/KUT/KT family, plays a major role in the cycling of K^+ and Na^+ from shoot to root in rice. OsHAK18 is expressed abundantly in rice mesophyll cells and CC complexes, functions in efficient utilization of K^+ and limiting Na^+ accumulation in the shoot, and contributes to source-to-sink translocation of K^+-accompanied soluble sugar for the production of grains.

RESULTS

Tissue and cellular localization of *OsHAK18* expression in rice

Plant HAK transporters have been shown to contribute to root K^+ uptake and translocation of K^+ from root to shoot under varied supply of [K^+]. By checking the expression pattern of rice HAK transporter genes via publicly released microarray data (RiceXPro, http://ricexpro.dna.affrc.go.jp/), we found that *OsHAK18*, unlike other HAK family members, is minimally transcribed in the root, suggesting that its function may divert from what is currently known about this family. Before exploring the physiological function of this gene, we first examined the organ-specific expression pattern of this gene by qRT-PCR in 3-week-old seedlings. Indeed, the transcript level is low in the root and leaf sheath but high in the leaf blade (Supplemental Figure S1A).

134 To examine further the tissue and cellular localization of this gene in rice, the GUS (β-
135 glucuronidase) reporter gene was fused to the putative promoter of *OsHAK18* (2000 bp
136 upstream of the translational start codon), and then transgenic rice plants harboring the
137 *ProOsHAK18:GUS* construct were generated. Histochemical analysis of these transgenic
138 rice plants showed that *OsHAK18* is expressed in the vascular cylinder of roots, basal
139 nodes and leaves, as well as in mesophyll cells (MCs; Supplemental Figure S1B, a-c;
140 Figure 1). OsHAK18 is also expressed in the glumous flower (Supplemental Figure S1Bd).
141 To further examine the expression of *OsHAK18* at a cellular level, an immunostaining
142 analysis was performed. In both roots and basal nodes, *OsHAK18* expression was
143 restricted to the phloem. Specifically, *OsHAK18* was expressed in the companion cells
144 (CCs) of the root phloem (Figure 1A, d and e) as well as in the phloem of the regular
145 vascular bundle (RVB) and enlarged vascular bundle (EVB; Figure 1B, c-e). Unlike that
146 found in roots and basal nodes, *OsHAK18* was expressed in both the phloem
147 parenchyma cells (PPCs) and CCs and xylem parenchyma cells (XPCs) of leaf sheaths
148 and leaf blades (Figure 1, Cc and Dc). Additionally, in leaf blades, it was also transcribed
149 in vascular bundle sheath (VBS) layer and MCs (Figure 1Dc).

150 OsHAK18 is located in the rice protoplast plasma membrane and 151 mediates K^+ and Na^+ transport in yeast

152 To determine the subcellular localization of OsHAK18, we transiently co-expressed in rice
153 protoplasts *OsHAK18* fused to *eGFP* at its N- or C-terminal, and *OsRac1* fused to
154 mCherry as the plasma membrane marker (Figure 2). eGFP alone, the product of an
155 'empty' vector, diffused within the cytosol, while the green signal of the eGFP-fused
156 OsHAK18 overlapped very well with the plasma membrane marker, irrespective of the
157 OsHAK18 terminus to which eGFP was fused (Figures 2, A and B).
158 To test whether OsHAK18 is a K^+ transporter, *OsHAK18* was expressed in yeast strain
159 G19. OsHAK18 increased by about 25% the Rb^+ content of G19 supplied with Rb^+ (Figure
160 2C). OsHAK18 also elevated K^+ and Na^+ content of G19 supplied with KCl and NaCl,
161 respectively (Figure 2C). These results suggest that OsHAK18 is able to transport both
162 Na^+ and K^+.

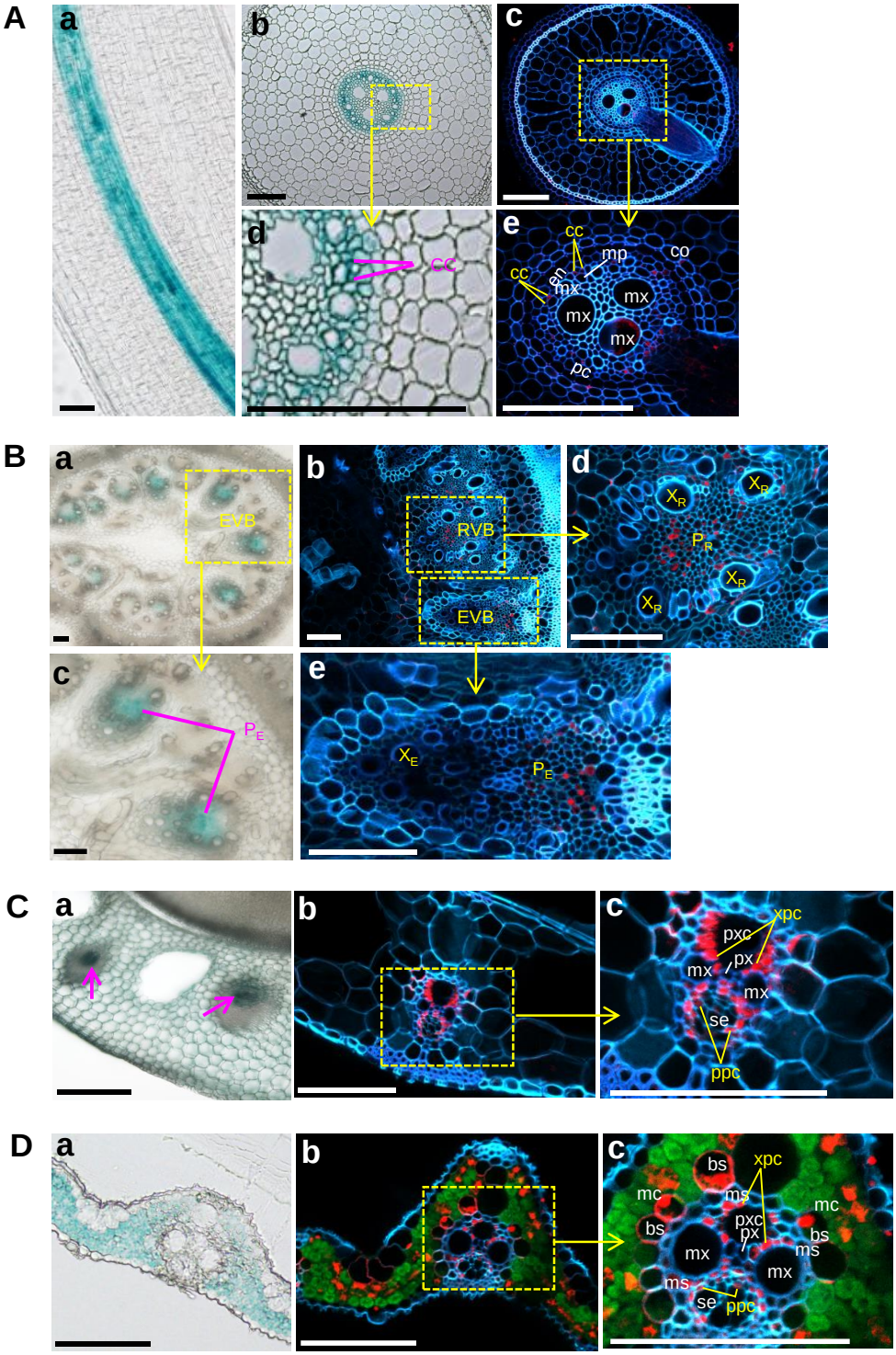

Figure 1. Tissue and cellular localization of *OsHAK18* in rice.

The localization is based on the detection of GUS reporter staining in transgenic rice plants harboring the *ProOsHAK18:GUS* construct and by *OsHAK18* immunostaining. A, crown root. B, basal node. C, leaf sheath. D, leaf blade. The GUS staining is seen in the transmitted-light images, Aabd, Bac, Ca,

Da. The immunostaining - in confocal fluorescence images, Ace, Bbde, Cbc, Dbc. In the immunostained cross sections, the red, green and blue colors represent the expression of *OsHAK18*, chlorophyll autofluorescence and cell wall autofluorescence, respectively. bs, vascular bundle sheath; cc, phloem companion cell; co, cortex; en, endodermis; ep, epidermis; EVB, enlarged vascular bundle; mc, mesophyll cell; mp, metaphloem; ms, mestome sheath; mx, metaxylem vessel; pc, pericycle; P_E, phloem of EVB; P_R, phloem of RVB; px, protoxylem; pxc, protoxylem cavity; RVB, regular vascular bundle; sc, sclerenchyma; se, sieve element; ppc, phloem parenchyma cell; X_E, xylem of EVB; xpc, xylem parenchyma cell; X_R, xylem of RVB. Scale bars = 100 μm.

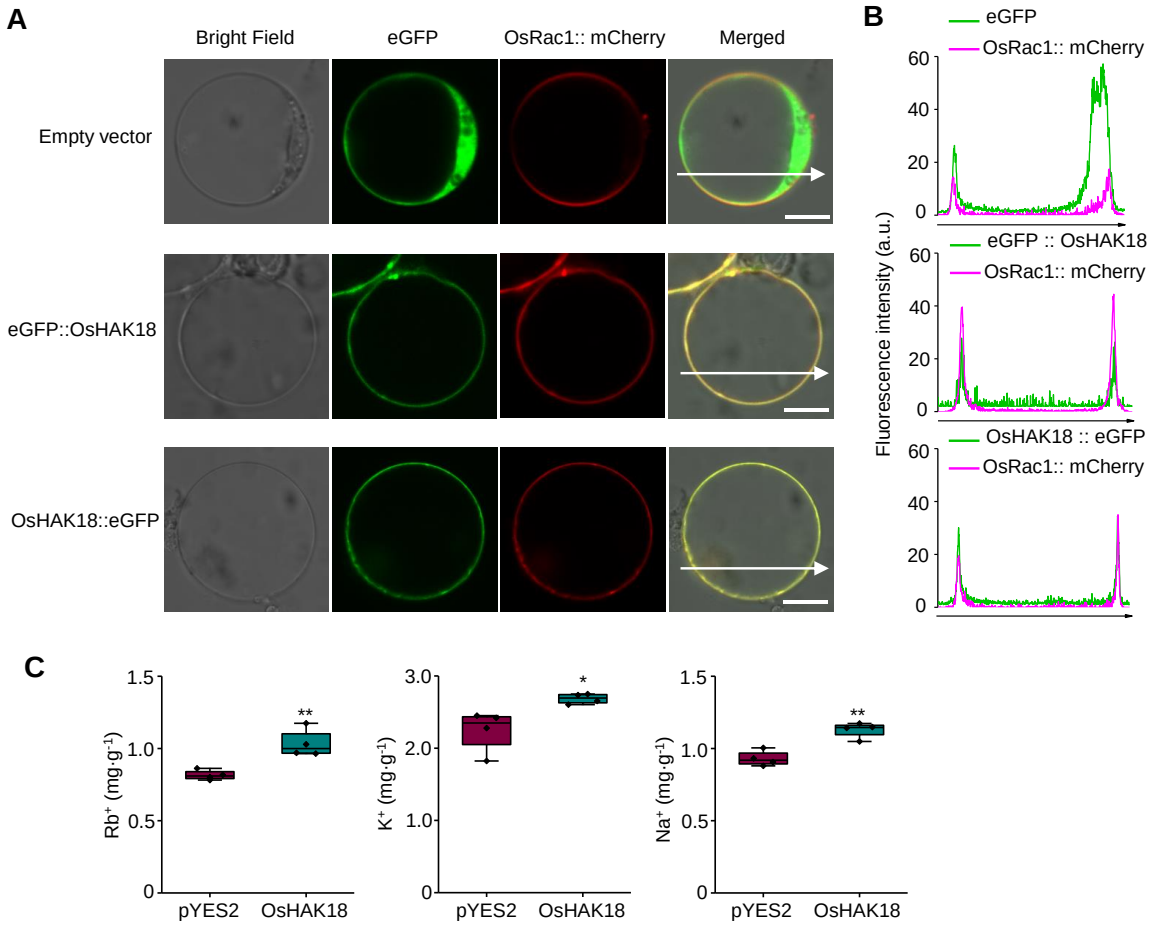

Figure 2. Subcellular localization of OsHAK18 and evaluation of the K^+ transport activity of OsHAK18 in yeast.

A, An expression of eGFP::OsHAK18 or OsHAK18::eGFP fusion proteins in rice protoplasts. OsHAK18 was co-localized with the plasma membrane-localized GTPase OsRac1. Scale bars = 10 μm. B, Line scans of rice protoplasts co-expressing OsHAK18–eGFP and OsRac1. C, Cells of G19 transformed with the empty vector pYES2 or OsHAK18 were cultured in liquid SC-U medium

supplemented with RbCl for 12 h, KCl or NaCl for 24 h. In the box plots, the symbols represent individual data, whiskers represent minimum and maximum data values, the boxes are delimited by the first and the third quartiles, and the horizontal line within the box indicates the median. Significant differences from pYES2 are indicated by asterisks (*, $P<0.05$; **, $P<0.01$). Non-paired, two-tailed, equal-variance t-test was used for the statistical analysis.

OsHAK18 affects significantly K^+ distribution between root and shoot

The GUS expression profile, subcellular location and the transport activity of OsHAK18 in G19 yeast suggest that OsHAK18 may mediate K^+ translocation in rice. To delve into the physiological function of this transporter, we obtained two different *Tos17* insertion mutants of *OsHAK18*-knockout (KO) in genetic background of cv. Nipponbare from NIAS institute in Japan and cv. Zhonghua11 from Huazhong Agricultural University in China, and verified their *Tos17* insertional sites (Supplemental Figure S2, A-C). In addition, we generated *OsHAK18* self-promoter-controlled overexpression lines (OX) in cv. Nipponbare (Supplemental Figure S2, D-F).

In the *OsHAK18*-KO lines, at the normal 1 mM external K^+ concentration ($[K^+]_{EXT}$), K^+ concentration was reduced in the root but not in the shoot (Figure 3A), while at 0.1 mM $[K^+]_{EXT}$, K^+ concentration was reduced in the root as well but was elevated appreciably in leaf sheath (Figure 3C). Altogether, *OsHAK18*-KO dramatically increased the accumulation of K^+ in shoot relative to root irrespective of the $[K^+]_{EXT}$ (Figure 3, E and G).

OsHAK18 function was also analyzed in three representative OX lines. While at an $[K^+]_{EXT}$ of 1 mM OX did not affect the K^+ concentration in the root and shoot (Figure 3B), at the low $[K^+]_{EXT}$ of 0.1 mM, OX increased $[K^+]$ in the root and decreased it in the leaf blade (Figure 3D). As expected, with 1 mM K^+ in the growth solution, OX did not affect also the relative distribution of K^+ between the shoot and the root (Figure 3F). In contrast, with 0.1 mM $[K^+]_{EXT}$, OX diminished the relative K^+ accumulation in the shoot (Figure 3H). These results suggest that under a limited K^+ supply OsHAK18 affects appreciably the distribution of K^+ between the root and the shoot.

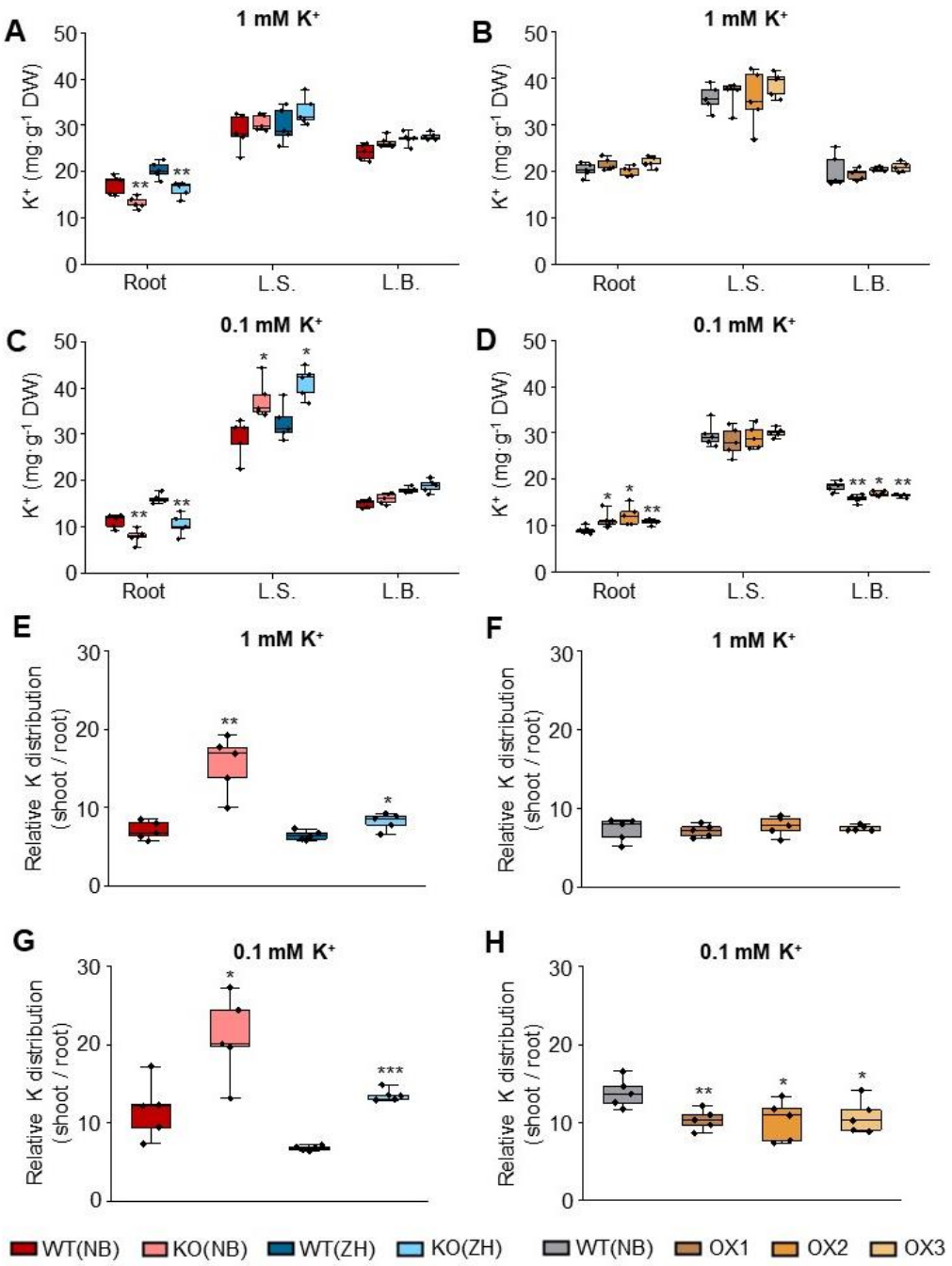

Figure 3. Effect of *OsHAK18* expression level on K^+ distribution at seedling stage.

Ten-day-old seedlings were grown in IRRI solution containing 1 mM K^+ for 4 weeks, then transferred to 1 mM K^+ (A, B, E, F) or to 0.1 mM K^+ (C, D, G, H) solutions for 2 weeks. A-D, K^+ concentration in root, leaf sheath (L.S.) and leaf blade (L.B.). E-H, Relative K^+ distribution (shoot / root). Detailed data of total K^+ content in root and shoot are provided in Supplemental Figure S3. The box plots and t-tests are as in Figure 2. Significant differences from the corresponding wild type (WT) are indicated by asterisks (*, $P<0.05$; **, $P<0.01$; ***, $P<0.001$).

OsHAK18 does not contribute to root K^+ uptake and transport from root to shoot

In the root, *OsHAK18* is expressed only in the stele, not in epidermal and cortex cells (Figure 1A, a-c), which suggested that OsHAK18 may not contribute to K^+ uptake. To test this, we determined the short-term K^+ acquisition rate (normalized to the root weight) at 1 mM or 0.1 mM [K^+] in the growth medium. The K^+ acquisition rate during 12-h of all the rice genotypes, WT, KO and OX was almost the same irrespective of the $[K^+]_{EXT}$ (Supplemental Figure S4). Thus, the results exclude a direct role of OsHAK18 in the root K^+ uptake in rice.

To examine the OsHAK18 function in the xylem or phloem transport of K^+, we first analyzed K^+ concentration in the xylem sap of all rice lines grown in 1 or 0.1mM K^+. To generate similar starting conditions for both treatments, we collected the xylem sap initially in 1h intervals for 3 consecutive hours while the roots remained in a medium without K^+, and subsequently – for additional 3 hs with either 1- or 0.1-mM K^+ restored to the bath. In the KO lines grown in 1 mM K^+, the xylem sap K^+ concentration was lower than in the corresponding WT only after the first h of K^+ deprivation (Figure 4A), while in KO grown in 0.1 mM K^+, the xylem sap K^+ concentration was lower than in the corresponding WT for the first two hs of K^+ deprivation (Figure 4B).

In the OX lines grown in 1 mM K^+, the xylem sap K^+ concentration was the same as in WT and did not change with time (Figure 4C), while in OX grown in 0.1 mM K, it was higher than in WT only at the first h of deprivation and then declined in both OX and WT during hours 2-3 of deprivation (Figure 4D). After K^+ was added back, K^+ concentration in xylem sap of KO or OX lines remained similar to the corresponding WTs and did not increase during the 3 hs of the follow up (Figure 4, A-D). These results support the notion that OsHAK18 does not mediate root K^+ uptake and does not contribute to K^+ translocation from root to shoot.

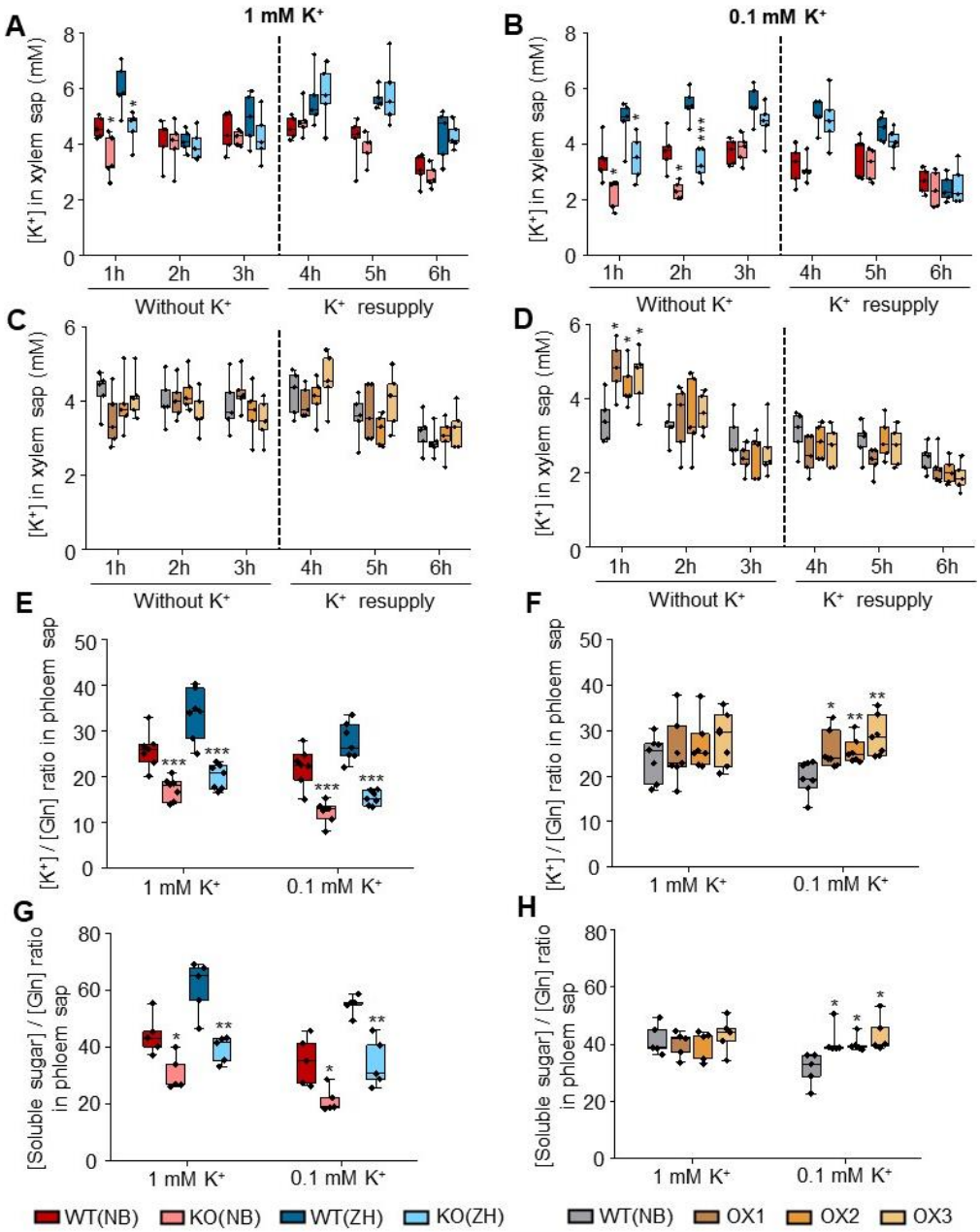

Figure 4. Effect of *OsHAK18* expression level on K^+ concentration in the xylem and soluble sugar concentration in phloem sap of rice.

A-D, The seedlings were grown in IRRI solution containing 1 mM K^+ for 8 weeks, then transferred to a medium with 1 mM K^+ (A and C) or 0.1 mM K^+ (B and D) for 3 days. Subsequently, the shoot was excised, the root was transferred to 0.1 mM $CaCl_2$ solution without K^+ and the xylem sap was collected during three one-hour periods. After 3 hs, the root was transferred back to 1 mM K^+ (A and C) or 0.1 mM K (B and D) solution and the xylem sap was collected similarly, in three 1-h periods for 3 more hours. E-H, The seedlings were grown in IRRI solution containing 1 mM K^+ for 8 weeks, then

transferred to a medium with 1 or 0.1 mM K^+. After 3 days of culture, phloem sap was collected during a 5-h period for K^+ and soluble sugar analysis. Glutamine was determined for internal standard (Ren *et al*., 2005). The box plots and t-tests are as in Figure 2. Significant differences from the corresponding WT are indicated by asterisks (*, $P<0.05$; **, $P<0.01$; ***, $P<0.001$).

OsHAK18 is involved in K^+ circulation and sugar translocation in phloem

Based on the above results, it is reasonable to assume that OsHAK18 influences K^+ root and shoot distribution via phloem transport. To clarify this, phloem sap was collected from all these rice lines grown in a medium with 1 mM or 0.1 mM $[K^+]_{EXT}$. Because glutamine is abundant in the phloem sap and remains quite constant during the entire 24 hs day-night cycle, glutamine is often used as an internal standard for measuring the concentration of ion and photo-assimilates in phloem sap (Corbesier et al., 2001; Ren et al., 2005). The phloem sap K^+ concentration was thus normalized to the glutamine concentration in the same sample. The phloem sap K^+ concentration in both KO lines was only about 50%-65% of that in the corresponding WTs irrespective of the $[K^+]_{EXT}$ levels (Figure 4E), while in all three OX lines grown in 0.1 mM $[K^+]_{EXT}$ it increased by at least 30% (Figure 4F). These results suggest that OsHAK18 contributes to K^+ entry into the phloem.

Since translocation of photo-assimilates from source leaves to roots in phloem requires high K^+ concentrations in the sieve tubes and a steep transmembrane pH gradient, we detected OsHAK18 effect on sugar concentration in the phloem. Remarkably, both KO or OX of *OsHAK18* had a similar effect on soluble sugar in the phloem at both low and normal K^+ supply level (Figure 4, G and H).

To test further whether OsHAK18 contributes to K^+ recycling from shoot to root, we took advantage of the Rb^+ transport capability of the HAK family transporters (Ródenas et al., 2017) and performed an experiment with split-root plants. One half-root was first exposed to 0.5 mM Rb^+ and the other half – to 0.5 mM K^+ for 3 hs. After that, the medium in both root containers was switched to one with 0.5 mM K^+ (Figure 5A). We measured the Rb^+ content in both parts of the root and the shoot at 3 hs and 6 hs after initiation of the treatments.

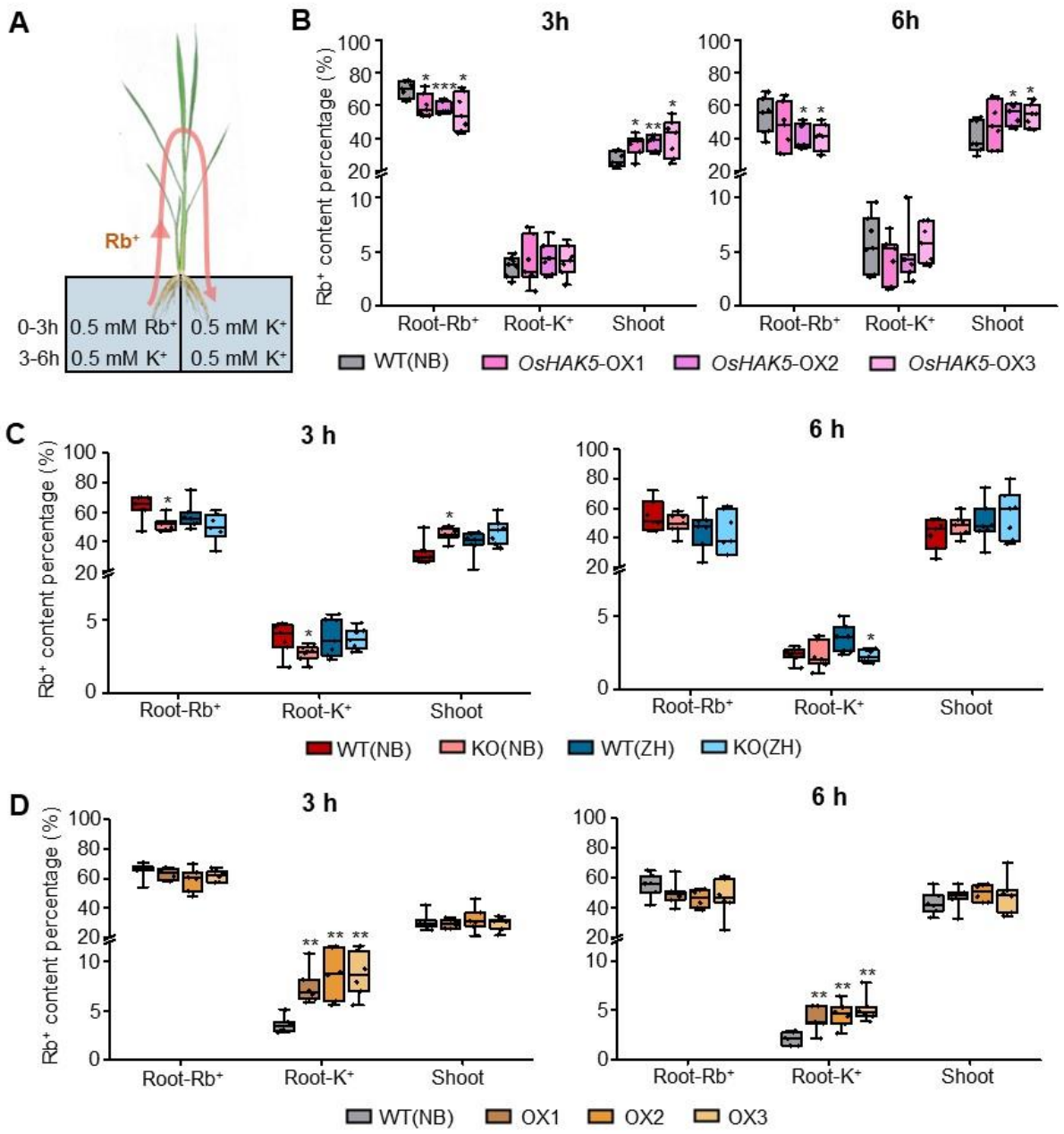

Figure 5. Effect of *OsHAK18* expression level on Rb^+ transport in rice plants.

A, Schematic diagram of split-root experiment. B, Rb^+ content percentage (i.e., the percentage of the total Rb^+ acquired by the plant) in different plant parts in *OsHAK5* overexpression lines and their corresponding WT at 3 h and 6 h of the pulse chase. C, *OsHAK18* KO lines and their corresponding WTs. D, *OsHAK18* overexpression lines and their corresponding WT. Root- Rb^+, Root exposed to Rb^+; Root- K^+, Root not exposed to Rb^+. The box plots and t-tests are as in Figure 2. Significant differences from the corresponding WT are indicated by asterisks (*, $P<0.05$; **, $P<0.01$; ***, $P<0.001$).

As a control, we performed the same experiment on rice overexpressing *OsHAK5*, a transporter known to mediate root to shoot K^+ translocation in rice. In *OsHAK5*-OX, as expected, the relative amount of Rb^+ in the Rb^+-exposed half root (i.e., the percentage of the total Rb^+ acquired by the plant) was lower than in WT, while in the roots exposed to K^+, the relative amount of Rb^+ was the same as in WT (Figure 5B). In the shoot, Rb^+ accumulation was enhanced in *OsHAK5*-OX relative to WT (Figure 5B). The fulfilled expectation with regard to the *OsHAK5*-OX effect, together with an earlier demonstration of Rb^+ transport by OsHAK18 (Figure 2C), confirmed that the Rb^+ distribution in the split-root experiment with OsHAK18 also reliably represents the circulation of K^+ in rice.

The relative amount of Rb^+ in the Rb^+-exposed half root was almost the same in both *OsHAK18*-KO lines and their corresponding WTs (roughly 50-60 %) except that in the NB KO line it was less than in NB WT in 3h of treatment. The root of the K^+-exposed half contained a very low fraction of Rb^+ (roughly 4% of total), KO reduced this even further (by roughly 25-30% of WT, the NB cultivar after 3 hs and the ZH cultivar after 6 hs; Figure 5C). In the shoot, which accumulated about 40% of the Rb^+ in 3 hs and 50% Rb^+ in 6 hs, the NB KO line accumulated more Rb^+ than NB WT in 3h of treatment (Figure 5C). In contrast, the Rb^+ content in the K^+ exposed roots of *OsHAK18*-OX lines were more than double that in WT at both hour 3 and hour 6 (Figure 5D). All these data support the notion that the direction of K^+ flow mediated by OsHAK18 is opposite from that of OsHAK5, and that OsHAK18 enhances K^+ translocation from shoot to root.

OsHAK18 alters the plant architecture and the sugar translocation resulting in an increased yield of rice in a paddy field

To reveal the role of OsHAK18 in the rice maturation stage, we evaluated the plant growth and the grain yield of WT, KO, and OX plants. Compared to WT, *OsHAK18*-KO plants had appreciably reduced height, tiller number, panicle length, seed setting rate (%) and grain number per panicle, leading to reduced yield and grain-to-straw ratio (Figure 6, A and B; Supplemental Figure S5, A and C). In contrast, while *OsHAK18*-OX plants had also reduced plant height, they had markedly higher tiller number and therefore, a higher grain yield (Figure 6, F and G; Supplemental Figure S5, B and D).

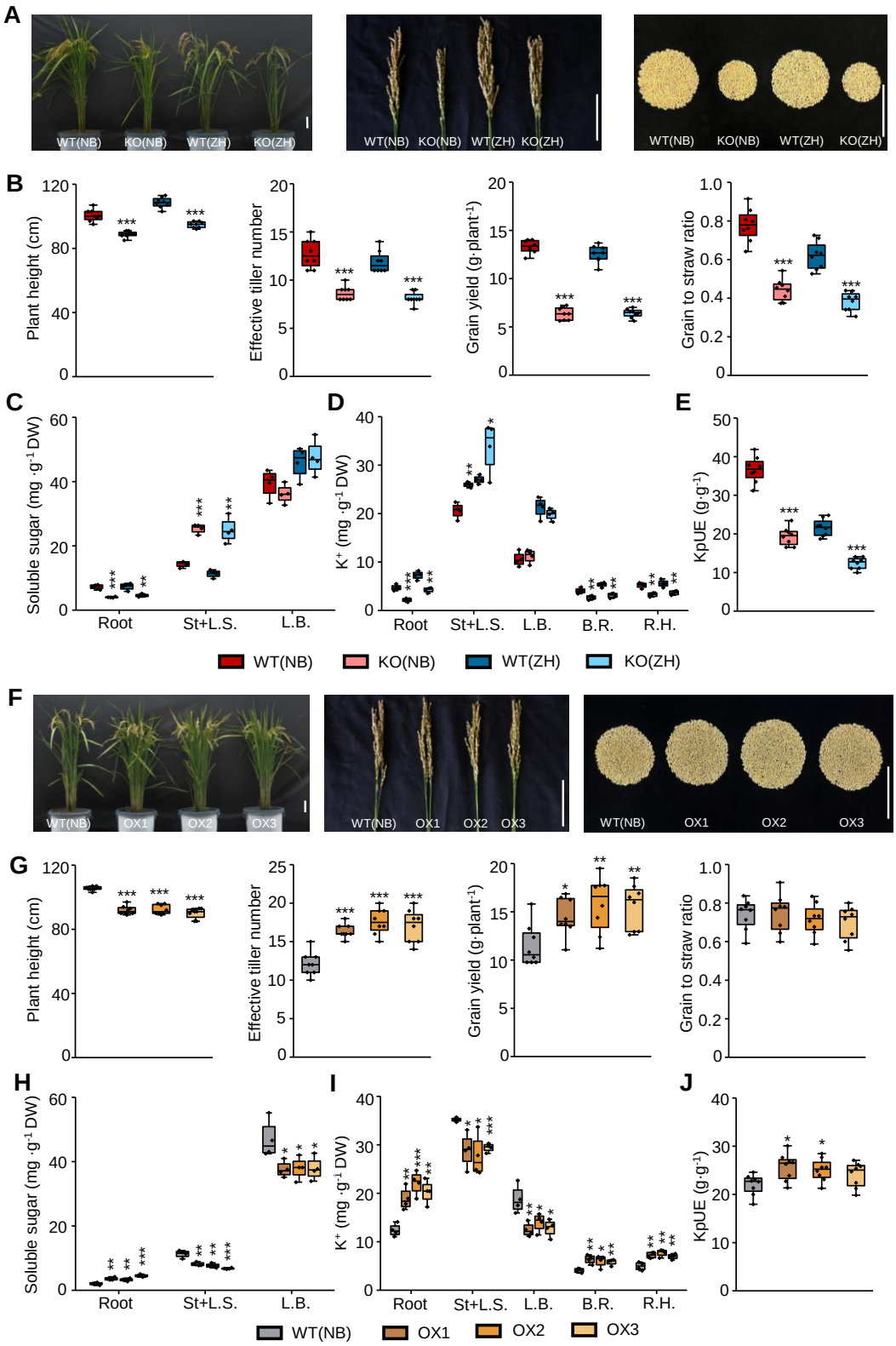

Figure 6. Effect of *OsHAK18* expression level on agronomic traits and K^+ and soluble sugar distribution at reproduction.

Rice plants were grown in the paddy field and irrigated, fertilized and medicated regularly until they are fully mature. A and F, Phenotypes of whole plants and panicles, and yield per plant. Scale bars = 10 cm. B and G, Plant height, effective tiller number, grain yield, grain to straw ratio. C and H, Soluble sugar concentration. D and I, K^+ concentration. E and J, KpUE, K^+ physiological utilization efficiency, i.e., the grain yield produced by unit weight of total accumulated K^+ per plant. St+L.S., Stem and leaf sheath; L.B., Leaf blade; B.R., Brown rice; R.H., Rice hull. Detailed data of other agronomic traits are provided in Supplemental Figure S5. The box plots and t-tests are as in Figure 2. Significant differences from the corresponding WT are indicated by asterisks (*, $P<0.05$; **, $P<0.01$; ***, $P<0.001$).

Since K^+-generated turgor pressure in the phloem is essential for the loading of soluble sugar at the source and unloading at sink sites (Dryer et al., 2017), we asked whether OsHAK18 had a role in these processes. Therefore, we examined the soluble sugar distribution in the root, stem, leaf sheath and leaf blade. In the *OsHAK18*-KO plants, soluble sugar accumulation in the root was markedly lower compared to WT, but in the stem and leaf sheath, it was higher than in the WT (Figure 6C). In contrast, in the *OsHAK18*-OX plants soluble sugar content was higher in the roots but lower in the stem, leaf sheath, and leaf blade in comparison with the WT (Figure 6H).

To further detect the OsHAK18 role in altering K^+ distribution between source and sink organs at the maturation stage, we measured K^+ concentration in the root, stem, leaf sheath, leaf blade, brown rice (a whole rice grain without the hull), and rice hull. As expected, K^+ concentration in the root, brown rice and rice hull was reduced by *OsHAK18*-KO and increased by *OsHAK18*-OX. In contrast, K^+ concentration in stem and leaves was increased by *OsHAK18*-KO and decreased by *OsHAK18*-OX (Figure 6, D and I). The differences in K^+ content among the samples were consistent with those of the sugar. Interestingly, K^+ physiological utilization efficiency (KpUE), i.e., the grain yield normalized (w/w) to the total accumulated K^+ in a plant, was almost halved by *OsHAK18*-KO (Figure 6E), but increased by 9% - 17% by *OsHAK18*-OX (Figure 6J), demonstrating that OsHAK18-controlled K^+ circulation in the phloem is essential for maintaining a high KpUE. Thus, properly enhancing the OsHAK18 activity driven by its endogenous promoter can promote both grain yield and K^+ use efficiency.

OsHAK18 mediates Na^+ recycling from shoot to root under salt stress

Since OsHAK18 enhanced also the accumulation of Na^+ in yeast, we examined its function in rice under 100 mM NaCl stress. *OsHAK18*-KO reduced both K^+ and Na^+ concentration in the root, while increasing the concentration of Na^+, but not K^+, in the shoot (Supplemental Figure S6, A and C). Their calculated K^+/Na^+ ratio was lower than in WT in both root and shoot (Supplemental Figure S6E). In contrast, *OsHAK18*-OX elevated K^+ concentration but decreased Na^+ concentration in the shoots with the opposite change of K^+ and Na^+ concentration in the root (Supplemental Figure S6, B and D), and thus resulted in a higher K^+/Na^+ ratio compared to WT in the shoot (Supplemental Figure S6F).

Ion recycling under high salt stress may be affected due to a disruption of phloem transport by plasmodesmata plugged by callose accumulation and P-protein aggregation at the sieve pores (Xie and Hong, 2011). To distinguish this effect of the salt stress on plasmodesmata transport from the effect of salt stress on membrane transport via the activity of the OsHAK18, we treated all rice lines with a moderate salt stress of 20 mM Na^+ for 3 days and measured K^+ and Na^+ in the phloem sap. Both K^+ and Na^+ concentrations were appreciably lower in the sap of the *OsHAK18*-KO plants than in WT (Figure 7, A and B), and markedly higher (by about 30-40 %) in the phloem sap of the *OsHAK18*-OX lines compared to WT (Figure 7, C and D). The results suggest that under salt stress, in rice, OsHAK18 enhances Na^+ (K^+) recycling from the shoot to the root.

In a follow-up experiment, after the 20 mM Na^+ treatment, we returned the plants to a normal medium for additional 3 days and then measured K^+ and Na^+ content in the roots and shoots. Although K^+ concentration and its relative distribution in shoots of KO and OX plants were similar to those of WT (Figure 7, E, G, I and K), Na^+ concentration in the leaf sheath and the leaf blade of KO plants was markedly higher than in the respective WT plants (Figure 7F). And furthermore, compared to WT, *OsHAK18*-KO plants had a lower fraction (% of total accumulated amount per plant) of Na^+ in the roots but a higher Na^+ fraction in the leaf blade (Figure 7J), and these differences were exactly opposite in the *OsHAK18*-OX plants (Figure 7L), resulted in decrease of K^+/Na^+ ratio in the shoot of *OsHAK18*-KO and an increase in the shoot of *OsHAK18*-OX. All these results indicate

that OsHAK18 contributes to the circulation of Na^+ relatively more than K^+ from shoot to root under salt stress.

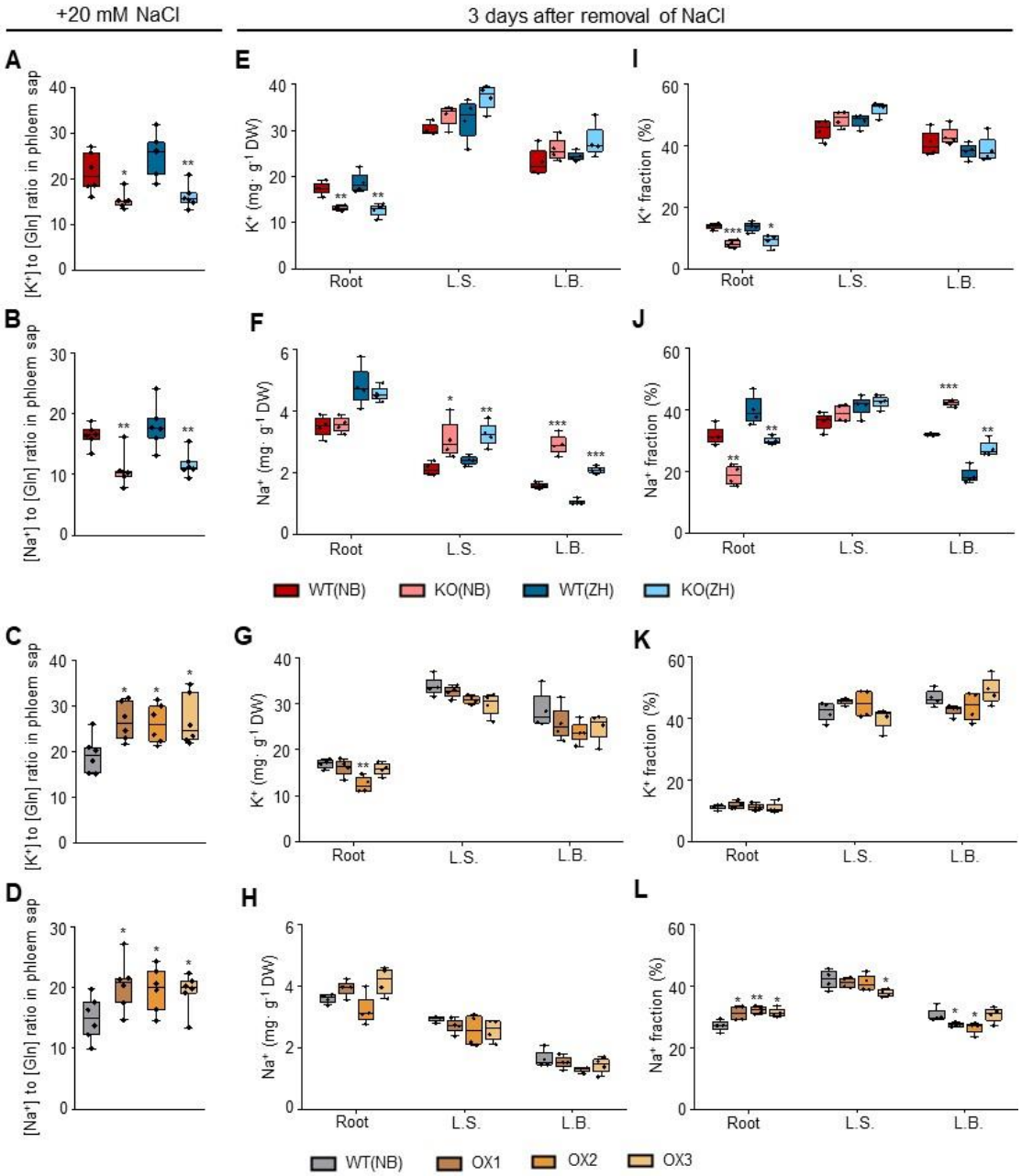

Figure 7. Effect of *OsHAK18* expression level on K^+ and Na^+ transport and distribution in rice supplied with NaCl in the culture solution.

Ten-day-old seedlings were grown in IRRI solution containing 1 mM K^+ for 4 weeks, then transferred to a solution containing additionally 20 mM NaCl and allowed to grow for 3 d. A-D, The phloem sap

was collected and analyzed. E-L, After 20 mM NaCl treatment for 3 d, seedlings were transferred to IRRI solution without NaCl for 3 days. K^+ or Na^+ fraction (%) represents the percentage of K^+ or Na^+ content in each plant part to the total K^+ or Na^+ content of the whole plant. L.S., Leaf sheath; L.B., Leaf blade. The box plots and t-tests are as in Figure 2. Significant differences from the corresponding WT are indicated by asterisks (*, $P<0.05$; **, $P<0.01$; ***, $P<0.001$).

DISCUSSION

That K^+ circulates in plants from root to shoot and then back from shoot to root has been already textbook knowledge for years. Out of the rice HAK/KUP/KT genes of K^+ carriers, the *OsHAK18* gene product, OsHAK18, is the first of its family to be shown here unequivocally to mediate the downward, shoot-to-root K^+ translocation via the phloem, and translocation of Na^+ under presence of Na^+ salts. Enhancing *OsHAK18* expression controlled by its native promoter can dramatically promote sugar translocation, grain yield and K^+ physiological utilization efficiency in rice (Figure 6, F-J).

The specific cellular localization of OsHAK18 suggests its role in several stages of this K^+ remobilization. In source leaves, OsHAK18 mediates the transport of K^+ from MCs to the sieve element-companion cell (SE-CC) complex (Figure 8A). The short-distance transport of K^+ in source leaves might achieve through three distinct but partially overlapped pathways: (i) K^+ leaked to the apoplastic space from MCs is imported into the adjacent MCs toward the vasculature, VBS, mestome sheath cells (MSCs), XPCs and PPCs/CCs, and then to phloem sieve element through plasmodesmata; (ii) K^+ in xylem vessel is unloaded into XPCs, and then (when lost to the apoplasm) reloaded into PPCs/CCs by OsHAK18, and finally arrives in sieve element through plasmodesmata; (iii) K^+ in the apoplasm between MSCs and neighboring PPCs is imported by OsHAK18 into the PPCs/CCs , and then arrives at sieve elements as well. In parallel, in the rice node, OsHAK18 mediates the influx of K^+ into PPCs/CCs of the EVB and regular/diffuse vascular bundle (RVB/DVB) (Figure 8B). In future work, it would be of interest and significance to identify the transporters responsible for K^+ efflux from several cell types in either leaves or nodes.

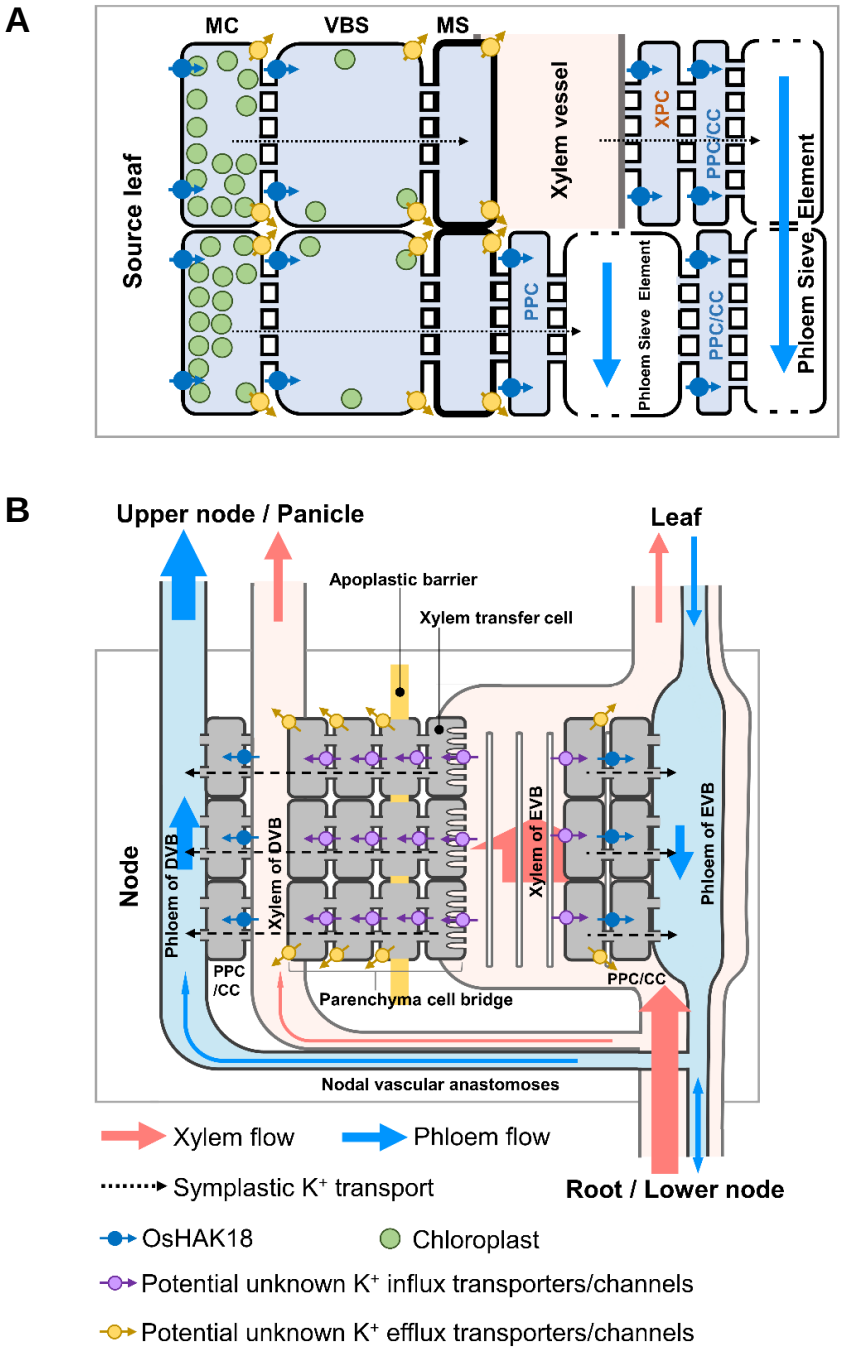

Figure 8. A working model for the roles of OsHAK18 in K^+ redistribution in the leaf blades and nodes of rice.

A, The role of OsHAK18 in the short distance transport of K^+ in a source leaf. B, The role of OsHAK18 in a node. CC, companion cell; DVB, diffuse vascular bundle; EVB, enlarged vascular bundle; MC, mesophyll cell; MS, mestome sheath cell; PPC, phloem parenchyma cell; VBS, vascular bundle sheath cell; XPC, xylem parenchyma cell. The size of arrows in the phloem and xylem represents flow area.

The evidence for OsHAK18 function in K^+ circulation in the phloem is based on an ensemble of 6 findings using a variety of approaches (all the comparisons are in relation to WT): (1) the natural *OsHAK18*-enriched expression in the plasma membrane of phloem CCs and PPCs (Figure 1; Figure 2, A and B); (2) a decreased K^+ accumulation in the root of *OsHAK18-KO* in both Nipponbare and Zhonghua11 cultivars (Figure 3, A and C) and especially the increased shoot-to-root ratio of [K^+] in the KO plants (Figure 3, E and G), and a decreased shoot-to-root ratio of [K^+] in *OsHAK18*-OX lines faced with K^+-deficient nutrient solution (Figure 3H); (3) identical rates of K^+ depletion from the media bathing the roots, irrespective of the K^+ supply level and plant genotype (this means an exclusion of OsHAK18 as a root K^+ acquisition transporter; Supplemental Figure S4); (4) a reduced [K^+] in the phloem sap of *OsHAK18*-KO plants (Figure 4E; Figure 7, A and B) and increased [K^+] in the phloem sap of *OsHAK18*-OX plants (Figure 4F; Figure 7, C and D); (5) the decreased Rb^+ translocation from the Rb^+-fed root half to the Rb^+-spared root half in a split root experiment in the KO plant (Figure 5C) and the enhanced Rb^+ translocation from the Rb^+-fed root part to the Rb^+-spared root part in the OX lines (Figure 5D); (6) the diametrically opposed to the above distribution of K^+ between the root parts of *OsHAK5*-OX in a control split-root experiment (Figure 5B), due to the known function of OsHAK5 in enhancing translocation of K^+ from root to shoot (Yang et al., 2014; 2020).

OsHAK18 is not involved in root K^+ absorption nor in root-to-shoot K^+ translocation

Root absorption of K^+ from culture medium is mediated by high- and low-affinity transporters and channels which enable adaptation to varied supply levels (Epstein et al., 1963; Maathuis and Sanders, 1997; Li et al., 2017). Root-acquired K^+ is transported into root stelar tissues and translocated from the root toward the shoot via xylem vessels (Marschner et al., 1996). As detected in Arabidopsis and rice, most of the putative HAK transporters and K^+ channels are located in root epidermal and xylem parenchyma cells, indicating their function mainly in root K^+ absorption and K^+ translocation to shoot. In Arabidopsis, AtHAK5 is the only system for root K^+ uptake from as low as 0.01 mM external [K^+] (Rubio et al., 2010), and AtKUP7 shows a higher expression level in root than other organs and is crucial for K^+ uptake (Han et al., 2016). In rice, both OsHAK1

467 and OsHAK5, which have the highest homology with AtHAK5, participate in K^+ absorption
468 and are up-regulated by K^+ deficiency in roots (Yang et al., 2014; Chen et al., 2015).
469 *OsHAK16* was also up-regulated by K^+ deficiency in roots and plays a similar but non-
470 redundant role in K^+ uptake by roots as do OsHAK1 and OsHAK5 (Feng et al., 2019). In
471 this study, we found that, unlike those already-described HAK-family members, *OsHAK18*
472 is expressed mainly in phloem CCs, but not in epidermal and cortex cells of the root
473 (Figure 1A), and its transcripts in the root are not up-regulated by K^+ deficiency
474 (Supplemental Figure S1A).

475 While in the long-term experiments *OsHAK18*-KO decreased the [K^+] in the root and
476 increased [K^+] in the shoot (Figure 3, A and C), the lack of effect of *OsHAK18* elimination
477 on the short-term K^+ absorption by the root (Supplemental Figure S4, A and B), indicates
478 that OsHAK18 is not involved in root K^+ uptake in rice. This conclusion is further
479 strengthened by the *OsHAK18*-OX under its native promoter that we generated to
480 enhance OsHAK18 activity without affecting its pattern of expression and localization to
481 avoid potentially alteration of its K^+ transport properties. As expected, *OsHAK18*-OX did
482 not affect the short-term K^+ absorption rate (Supplemental Figure S4, C and D). A similar
483 conclusion is also suggested by the lack of effect of either *OsHAK18*-KO or *OsHAK18*-
484 OX on the K^+ concentration in the xylem sap, irrespective of the external K^+ supply levels
485 at the root (Figure 4, A-D). However, in addition to phloem, *OsHAK18* is also expressed
486 in XPCs of leaf sheath and blade (Figure 1, Cc and Dc), similar to *OsHAK1*, *OsHAK5* and
487 *OsHAK16* (Yang et al., 2014; Chen et al., 2015; Feng et al., 2019), and therefore one
488 cannot completely rule out a potential function of OsHAK18 in the xylem delivery of K^+
489 from root to shoot masked by other K^+ transporters and channels.

490 OsHAK18 promotes K^+ circulation from shoot to root and sugar 491 translocation from source to sink organs

492 In plants, up to 90% of K^+ transported from root via xylem to aerial parts recycles back to
493 the root through the phloem along with photosynthates, sugars and other nutrients (Lu et
494 al., 2005; Peuke et al., 2011), which enables the shoot to communicate its nutrient
495 demand to the root (Dreyer et al., 2017) and avoid excess of cation (K^+). K^+ gradients
496 serve as a mobile energy source in plant vascular tissues and K^+ circulating in the phloem

transports energy stored in the K^+ gradient between phloem cytosol and the apoplast (Gajdanowicz et al., 2010; Dreyer et al., 2017). In Arabidopsis, a “weakly-inward rectifying” K^+ channel, AKT2, has been shown to mediate K^+ phloem loading, but also (under different circumstances) to mediate K^+ release from the phloem, thereby enhancing the loading of phloem with sugar (Deeken et al., 2002, Gajdanowicz et al., 2010). Similar to the AKT2, OsAKT2 has been shown to be important for K^+ phloem loading and K^+ recirculation via phloem (Tian et al., 2021). However, it was not known if additional K^+ transporter(s) is also involved in K^+ movement in the phloem, especially in the K^+ translocation from shoot to root. The fact that *OsHAK18*-KO plants are impaired in K^+ recirculation means that OsAKT2 cannot fulfill this role all by itself. OsHAK18 has now been revealed as a new participant in the phloem loading of K^+ and in the shoot-to-root translocation of K^+. Furthermore, OsHAK18’s participation in sugar translocation paralleling with K^+ redistribution (Figure 4, G and H; Figure 6, C and H) resembles the function of OsAKT2 which enhances sugar transfer from source sites to sink sites (Tian et al., 2021), demonstrating that OsHAK18 coordinates high delivery of K^+ and photo-assimilates in the phloem.

OsAKT2 and OsHAK18 may play complementary roles in phloem movement of K^+ at different K^+ supply levels or different loading directions. On one hand, OsAKT2 functions mainly as an inward rectifier with strong voltage-dependency (Huang et al., 2021) and the elimination of phloem-located *OsAKT2* expression resulted in relatively higher accumulation of K^+ in the shoot at a normal K^+ supply (Tian et al., 2021). Notably, OsHAK18 contributes to K^+ re-circulation in phloem at both normal and low K^+ supply status (Figure 3, E and H; Figure 4, E and F). In addition, in Arabidopsis, OsAKT2 can complement the K^+ deficiency in the phloem sap and leaves of *akt2* mutant (Huang et al., 2021). On the other hand, however, unlike AKT2 which functions in the leakage of K^+ from the companion cells of the transport phloem (Deeken et al., 2002; Gajdanowicz et al., 2010), OsAKT2 does not allow K^+ leak from cells (Huang et al., 2021). Furthermore, since this outward K^+ leak is what allows the Arabidopsis AKT2 to generate the sugar-loading-into-phloem “K^+ battery” (Gajdanowicz et al., 2010), the lack of outward K^+ leak via OsAKT2 casts doubt on its participation in any such battery in rice (Huang et al., 2021). Therefore, it seems that in the rice plant OsAKT2 and OsHAK18 share together the

528 responsibility for K^+ loading into the phloem, but between the two, only OsHAK18 is likely
529 to be involved in the phloem sugar loading, perhaps "partnering" instead with a dedicated
530 K^+ release channel, such as OsGORK (that is expressed in rice more widely than its
531 homolog, OsSKOR; Kim et al., 2015).

532 Enhancing OsHAK18 expression increases K^+ physiological utilization 533 efficiency and grain yield

534 Improving K^+ physiological use efficiency, i.e., less K^+ demand for reaching high yield, can
535 reduce soil K^+ depletion by plants and the demand for K^+ fertilizers (Shin, 2014). Unlike
536 N and P which is mainly accumulated in grains/seeds, the majority of acquired K^+ from
537 soil or fertilizer is kept in vegetative organs, like straw, in rice. The dramatic reduction of
538 K^+ concentration in the straw of *OsHAK18*-OX (Figure 6I) and its increased grain yield
539 (Figure 6G) signify an increase of K^+ physiological utilization efficiency by a non-negligible
540 9-17% (Figure 6J), resulting – we presume – from an enhanced circulation of K^+ in the
541 phloem.

542 We noticed that OsHAK18 had significant effect on rice architecture, especially tiller
543 number which is one of three major components in determining the rice grain yield (Figure
544 6, B and G; Supplemental Figure S5). Plant architecture including rice tiller number is
545 regulated by polar auxin transport (Lu et al., 2015; Luo et al., 2020). Cellular auxin fluxes
546 are strongly affected by transmembrane pH gradients (Steinacher et al., 2012), which, in
547 turn, are regulated by interactions between H^+ pumps, H^+-coupled carriers and ion
548 channels at the PM (Sze and Chanroj, 2018). For example, OsHAK5, an electrogenic
549 K^+/H^+ symporter, regulated the chemiosmotic gradient, PM polarization, and extracellular
550 pH in rice, resulting in positive regulation of polar auxin delivery streams and an increased
551 rice tiller number (Yang et al., 2020). Since OsHAK18 is a plasma-membrane-located
552 K^+/H^+ co-transporter (Figure 2), expressed abundantly in the vascular tissue (Figure 1B),
553 we speculate that OsHAK18 affects the pH in the apoplast, and thus, among others,
554 controls tiller emergence in the basal node, thus affecting rice architecture (Figure 6, B
555 and G). These findings may in the future render OsHAK18 a target for manipulations
556 aimed at increasing the rice yield and K^+ use efficiency in the field.

557

MATERIALS AND METHODS

Plant materials and growth conditions

Two cultivars of rice (*Oryza sativa* subsp. *japonica*) were used in this work, Nipponbare (NB) and Zhonghua11 (ZH). For hydroponic experiments, seed sterilization and basal nutrient solution composition for seedling growth were described previously (Ai et al., 2009). Similar-size ten-day-old rice seedlings of each wild-type (WT) and transgenic lines were selected and transferred to IRRI nutrient solution (Yoshida et al., 1976; Yang et al., 2014). For K^+ starvation or depletion experiments, rice seedlings were grown in the IRRI solution containing 1 mM K^+ for 4 weeks and then transferred into a solution in which KH_2PO_4 and K_2SO_4 were replaced by NaH_2PO_4 and KCl, respectively. For salt stress experiments, 100 mM NaCl was added in the IRRI solution after 4 weeks. In all treatments, the solutions were replaced every 2 days. The hydroponic experiments were carried out in a greenhouse with a 16h-light/8h-dark, temperature between 22-30℃, and 60% to 70% relative humidity. For field experiments, rice plants were grown in paddy soil with regular fertilization during the normal growing seasons in Nanjing, China. At each harvest, roots of all rice plants were washed in 0.1 mM $CaSO_4$ for 5 min. Roots, stems, leaf sheaths and blades, brown rice and rice hull were separated before their biomass was recorded and concentrations of K^+ and Na^+ were measured as described previously (Ding et al., 2006; Yang et al., 2014).

RNA extraction and transcript analysis of *OsHAK18*

Isolation of total RNA was extracted from roots, leaf sheaths and blades of treated seedlings with RNAiso plus reagent (TaKaRa, TaKaRa Bio Inc., Dalian, China) following the manufacturer's instructions. Relative quantitative results were normalized to *OsACT* (accession number AB047313) and are presented here as mean normalized transcript levels obtained by the comparative cycle threshold method ($2^{-\Delta\Delta Ct}$). Real-time PCR assays were performed in 20 μL reaction volumes using a QuantStudio 6 flex Real-time PCR system (Applied Biosystems). The primers used are listed in Supplemental Table S1.

GUS staining and immunostaining analysis

The 2000-bp DNA sequence upstream of the start codon of *OsHAK18* was amplified by PCR and the primers used are listed in Supplemental Table S2. The purified PCR product was then fused upstream of the *GUSPlus* reporter gene in pCAMBIA1300-GN vector via BamHI / KpnI (Chang et al., 2019). The construct was transformed into Agrobacterium strain EHA105 by electroporation, and then transformed into callus derived from mature embryos of japonica rice cultivar Nipponbare via Agrobacterium tumefaciens-mediated transformation (Jia et al., 2011). The GUS staining analysis was performed as described in Ai et al. (2009). Immunostaining analysis with an antibody against GUS was performed as described in Yamaji and Ma (2007), and sections were observed by a confocal laser scanning microscope (Leica, Wetzlar, Germany; TCS SP8X). The cell wall autofluorescence was excited by ultraviolet light with an intensity of 0.7%–3%; the collection bandwidth and gain value were 410–470 nm and 30%–60%, respectively. The collection bandwidth for Alexa Fluor 555 (the secondary antibody) was 560–580 nm, and the gain value was 50%–60% (Dai et al., 2022).

Subcellular localization assay

For constructing *eGFP*::*OsHAK18* and *OsHAK18*::*eGFP*, the *OsHAK18* coding sequence (including the stop codon) was amplified by PCR using primers listed in Supplemental Table S3. The amplified cDNA was cloned into the middle vector pSAT6A-EGFP-C1 and pSAT6A-EGFP-N1. The middle vector was cut by the PI-PspI and inserted in-frame into the expression vector pRCS2-ocs-nptII. OsRac1-mCherry was used as a plasma membrane control. Transient expression of *OsHAK18* in rice protoplasts, and fluorescence microscopy imaging observation using sequential scanning mode of confocal microscopy (TCS SP8X, Leica, Germany). Excitation/emission wavelengths were 488 nm/498–540 nm for eGFP and 552 nm/600–640nm for mCherry (Dai et al., 2022).

Yeast strains and culture conditions

OsHAK18 coding sequence was cloned into the expression vector pYES2, which contains the inducible GAL1 promoter, for selection and expression in yeast (*Saccharomyces cerevisiae*). The primers used are listed in Supplemental Table S4. The expression vectors were transformed into the Na^+-hypersensitive G19 (*MATα*, *his3*, *leu2*, *ura3*, *trp1*,

617 *ade2* and Δena1::HIS3::Δena4) strain (Quintero et al., 1996) of the yeast using the
618 LiAC/ssDNA/PEG method. The transformants were selected on Glc-containing SC-agar
619 plates without uracil (SC-U). For liquid culture of G19, we collected cells at 12 h in 5 mM
620 RbCl and 24 h in 400 mM KCl or NaCl SC-U mediums for Rb^+, K^+ and Na^+ measurement
621 (Feng et al., 2019).

622 Identification of *oshak18* mutant lines and generation of *OsHAK18*-
623 overexpressing transgenic rice

624 Two different *Tos17* insertion lines of *OsHAK18* knockout mutants in the genetic
625 backgrounds of cv. Nipponbare and cv. Zhonghua11 were requested from NIAS institute,
626 Japan and Huazhong Agricultural University, China, respectively. According to the
627 insertional information, two primers for *OsHAK18* gene and primers specifically for *Tos17*
628 vector were used to determine the *Tos17* insertional sites. Homozygous plants for *Tos17*
629 insertions were identified by two-round RT-PCR analysis (Supplemental Table S5).
630 Further detection of the expression levels of *OsHAK18* in the homozygous mutant
631 seedlings were performed by RT-PCR analysis.

632 For generating the transgenic rice lines with overexpression of the *OsHAK18* gene, the
633 endogenous promoter of *OsHAK18* (1958 bp sequence upstream of transcriptional start
634 site) was used to replace the ubiquitin promoter in the expression vector pTCK303 (Ai et
635 al., 2009), and the primers used are listed in Supplemental Table S6. Vector harboring
636 *pOsHAK18:OsHAK18* was transferred into *A. tumefaciens* strain EHA105 by
637 electroporation, and the agrobacteria were used to infect callus induced from WT rice (cv.
638 Nipponbare) as described in Tang et al. (2012). A total of 12 *OsHAK18*-OX transgenic
639 lines were selected after GUS staining and PCR analysis by following the protocol
640 described by Yang et al. (2014). Three representative lines (OX1, OX2, OX3) were used
641 for the detailed analysis (Supplemental Figure S2, E and F).

642 Measurement of K^+ and Na^+ concentrations in xylem sap and phloem
643 sap

644 Similar-size 10-day-old rice seedings of each WT and transgenic lines were grown in the
645 IRRI solution for 8 weeks and then transferred to 1- or 0.1-mM K^+ solutions for 3 days

646 before the sampling. The detailed protocols for the shoot excision, the xylem sap
647 collection by cotton ball, and the determination of K^+ concentration were described
648 previously by Yang et al. (2014). At the same time, the shoot part removed from plants
649 during the collection of the xylem sap was put into a calibrated test tubes containing 20
650 mL 20 mM EDTA solution (pH=7.5-8.0), and placed in dark environment with air humidity
651 higher than 70% for 5 hours to collect the phloem sap. The protocol was derived from
652 King and Zeevaart (1974). The amounts of K^+, Na^+ and glutamine released in the EDTA
653 solutions were determined by ICP-OES (Agilent 710, Agilent Technologies, USA) and
654 Agilent 1200 HPLC coupled with Agilent G6410 mass spectra, respectively. The K^+ or Na^+
655 to glutamine concentration ratio was used to standardize the K^+ or Na^+ data (Ren et al.,
656 2005).

657 Detecting the effect of *OsHAK18* expression level on the rice root short-
658 term K^+ acquisition

659 Rice K^+ depletion experiments followed the previously described procedures (Nieves-
660 Cordones et al., 2007; Rubio et al., 2008) with some modifications. Similar-size 10-day-
661 old rice seedlings were grown in the IRRI solution containing 0.1- or 1-mM K^+ for 4 weeks,
662 and then subjected to K^+ starvation for 7 days by excluding K^+ from both solutions. After
663 7 days of K^+ starvation, the roots were rinsed with a cold K^+-free nutrient solution, and
664 then seedlings of WTs or transgenic lines were transferred to containers filled with 350
665 mL of solution for 0.1- or 1-mM K^+ treatment (two plants per container). Three mL of the
666 solution were collected from each container at 0, 0.5, 1, 2, 4, 6, 8 and 12 h and K^+
667 concentration in the sample was determined by ICP-OES (Agilent 710, Agilent
668 Technologies, USA) as described previously (Cai et al., 2012). At the end of the
669 experiment, root fresh weight of each plant was determined. K^+ acquisition rate was
670 calculated by taking the amount of K^+ decrease in the solution at every time point and
671 normalizing it to the root fresh weight (g) of the corresponding individual plant (Chen et
672 al., 2015).

673 Split-root experiment for assay of Rb^+ circulation

674 Similar-size 10-day-old rice seedings of each WT and transgenic lines were grown in the

675 IRRI solution for 6 weeks. Then, the rice plants were grown individually in pots, and the
676 roots per plant were divided almost equally into two plastic vessels containing a nutrient
677 solution of 0.5 mM Rb^+ (Root-Rb^+) and 0.5 mM K^+ (Root-K^+), respectively. After 3 hours,
678 both roots were placed back into 0.5 mM K^+ nutrient solution for another 3 hours. The two
679 root parts and the shoots were collected at 3 h and 6 h, counting from the beginning of
680 Rb^+ treatment and their Rb^+ content was measured by ICP-MS (Thermo Fisher Scientific,
681 USA).

682 **Measurement of soluble sugar content**

683 Roots, stems, leaf sheaths and blades of soil-grown plants were harvested at the mature
684 stage. All samples were snap-frozen in liquid nitrogen and stored at -80℃. Soluble sugar
685 was extracted with 80% (v/v) ethanol from 80℃ water bath. Soluble content was
686 determined based on the method described by Leyva et al. (2008) with minor
687 modifications and were detected by anthrone-sulfuric acid colorimetry. The anthrone
688 reagent was prepared right before analysis by dissolving 0.1 g of anthrone (0.1%) in 100
689 mL of 70% (v/v) sulfuric acid, protected from light and used within 12 h. The reaction liquid
690 is heated and then cooled to room temperature before reading absorbance at 625 nm.

691 **Statistical analysis**

692 Data were analyzed by non-paired, two-tailed, equal-variance t-test using the SPSS 21
693 program (SPSS Inc., Chicago, IL, USA).

694 **Acknowledgements**

695 This work was supported by National Key Research and Development Program of China
696 (grant no. 2021YFF1000402-1) and National Natural Science Foundation of China (grant
697 no. 31872166).

698 **Data availability**

699 The data that support the findings of this study are available from the corresponding
700 authors upon reasonable request.

701 **Disclosures**

The authors have no conflicts of interest to declare.

Author contributions

L.Y. and G.X. conceived the study and designed the experiments; L.P. conducted most of the experiments; H.X., R.L. and Y.Z. generated transgenic lines and performed part of the experiments; M.G. conducted the immunostaining assay; L.Y., G.X., N.M. and L.P. analyzed the data and prepared the manuscript.

Supplemental data

Supplemental data associated with this article can be found in the online version.

Supplemental Figure S1. *OsHAK18* expression and tissue localization in rice.

Supplemental Figure S2. Homozygous *Tos17* insertion mutants of *OsHAK18* gene in rice and characterization of *OsHAK18*-overexpressing (OX) transgenic rice lines in the background of the Nipponbare cultivar.

Supplemental Figure S3. Effect of *OsHAK18* expression level on total K^+ content at the seedling stage.

Supplemental Figure S4. Effect of *OsHAK18* expression level on short-term root K^+ acquisition rates at different K^+ supply conditions.

Supplemental Figure S5. Effect of *OsHAK18* expression level on agronomic traits at reproduction.

Supplemental Figure S6. Effect of *OsHAK18* expression level on salt sensitivity of rice.

Supplemental Table S1. Primers used to amplify *OsACT* and *OsHAK18* for quantitative real-time PCR.

Supplemental Table S2. Primers used to amplify *OsHAK18* promoter for tissue localization.

Supplemental Table S3. Primers used to amplify *OsHAK18* cDNA for subcellular localization.

Supplemental Table S4. Primers used to amplify *OsHAK18* cDNA for functional assay in yeast.

Supplemental Table S5. Primers for identification two homozygous mutant lines of *oshak18*.

731 **Supplemental Table S6.** Primers used to amplify *OsHAK18* promoter and cDNA for
732 construction of over-expression.
733

734 LEGENDS OF FIGURES

735 **Figure 1. Tissue and cellular localization of *OsHAK18* in rice.**
736 The localization is based on the detection of GUS reporter staining in transgenic rice
737 plants harboring the *ProOsHAK18:GUS* construct and by *OsHAK18* immunostaining. A,
738 crown root. B, basal node. C, leaf sheath. D, leaf blade. The GUS staining is seen in the
739 transmitted-light images, Aabd, Bac, Ca, Da. The immunostaining - in confocal
740 fluorescence images, Ace, Bbde, Cbc, Dbc. In the immunostained cross sections, the red,
741 green and blue colors represent the expression of *OsHAK18*, chlorophyll
742 autofluorescence and cell wall autofluorescence, respectively. bs, vascular bundle sheath;
743 cc, phloem companion cell; co, cortex; en, endodermis; ep, epidermis; EVB, enlarged
744 vascular bundle; mc, mesophyll cell; mp, metaphloem; ms, mestome sheath; mx,
745 metaxylem vessel; pc, pericycle; P_E, phloem of EVB; P_R, phloem of RVB; px, protoxylem;
746 pxc, protoxylem cavity; RVB, regular vascular bundle; sc, sclerenchyma; se, sieve
747 element; ppc, phloem parenchyma cell; X_E, xylem of EVB; xpc, xylem parenchyma cell;
748 X_R, xylem of RVB. Scale bars = 100 μm.

749 **Figure 2. Subcellular localization of OsHAK18 and evaluation of the K^+ transport**
750 **activity of OsHAK18 in yeast.**
751 A, An expression of eGFP::OsHAK18 or OsHAK18::eGFP fusion proteins in rice
752 protoplasts. OsHAK18 was co-localized with the plasma membrane-localized GTPase
753 OsRac1. Scale bars = 10 μm. B, Line scans of rice protoplasts co-expressing OsHAK18–
754 eGFP and OsRac1. C, Cells of G19 transformed with the empty vector pYES2 or
755 OsHAK18 were cultured in liquid SC-U medium supplemented with RbCl for 12 h, KCl or
756 NaCl for 24 h. In the box plots, the symbols represent individual data, whiskers represent
757 minimum and maximum data values, the boxes are delimited by the first and the third
758 quartiles, and the horizontal line within the box indicates the median. Significant
759 differences from pYES2 are indicated by asterisks (*, $P<0.05$; **, $P<0.01$). Non-paired,
760 two-tailed, equal-variance t-test was used for the statistical analysis.

761 **Figure 3. Effect of *OsHAK18* expression level on K^+ distribution at seedling stage.**
762 Ten-day-old seedlings were grown in IRRI solution containing 1 mM K^+ for 4 weeks, then
763 transferred to 1 mM K^+ (A, B, E, F) or to 0.1 mM K^+ (C, D, G, H) solutions for 2 weeks. A-
764 D, K^+ concentration in root, leaf sheath (L.S.) and leaf blade (L.B.). E-H, Relative K^+
765 distribution (shoot / root). Detailed data of total K^+ content in root and shoot are provided
766 in Supplemental Figure S3. The box plots and t-tests are as in Figure 2. Significant
767 differences from the corresponding wild type (WT) are indicated by asterisks (*, $P<0.05$;
768 **, $P<0.01$; ***, $P<0.001$).

769 **Figure 4. Effect of *OsHAK18* expression level on K^+ concentration in the xylem and**
770 **soluble sugar concentration in phloem sap of rice.**
771 A-D, The seedlings were grown in IRRI solution containing 1 mM K^+ for 8 weeks, then
772 transferred to a medium with 1 mM K^+ (A and C) or 0.1 mM K^+ (B and D) for 3 days.
773 Subsequently, the shoot was excised, the root was transferred to 0.1 mM $CaCl_2$ solution
774 without K^+ and the xylem sap was collected during three one-hour periods. After 3 hs, the
775 root was transferred back to 1 mM K^+ (A and C) or 0.1 mM K (B and D) solution and the
776 xylem sap was collected similarly, in three 1-h periods for 3 more hours. E-H, The
777 seedlings were grown in IRRI solution containing 1 mM K^+ for 8 weeks, then transferred
778 to a medium with 1 or 0.1 mM K^+. After 3 days of culture, phloem sap was collected during
779 a 5-h period for K^+ and soluble sugar analysis. Glutamine was determined for internal
780 standard (Ren *et al*., 2005). The box plots and t-tests are as in Figure 2. Significant
781 differences from the corresponding WT are indicated by asterisks (*, $P<0.05$; **, $P<0.01$;
782 ***, $P<0.001$).

783 **Figure 5. Effect of *OsHAK18* expression level on Rb^+ transport in rice plants.**
784 A, Schematic diagram of split-root experiment. B, Rb^+ content percentage (i.e., the
785 percentage of the total Rb^+ acquired by the plant) in different plant parts in *OsHAK5*
786 overexpression lines and their corresponding WT at 3 h and 6 h of the pulse chase. C,
787 *OsHAK18* KO lines and their corresponding WTs. D, *OsHAK18* overexpression lines and
788 their corresponding WT. Root- Rb^+, Root exposed to Rb^+; Root- K^+, Root not exposed to
789 Rb^+. The box plots and t-tests are as in Figure 2. Significant differences from the
790 corresponding WT are indicated by asterisks (*, $P<0.05$; **, $P<0.01$; ***, $P<0.001$).

Figure 6. Effect of *OsHAK18* expression level on agronomic traits and K^+ and soluble sugar distribution at reproduction.

Rice plants were grown in the paddy field and irrigated, fertilized and medicated regularly until they are fully mature. A and F, Phenotypes of whole plants and panicles, and yield per plant. Scale bars = 10 cm. B and G, Plant height, effective tiller number, grain yield, grain to straw ratio. C and H, Soluble sugar concentration. D and I, K^+ concentration. E and J, KpUE, K^+ physiological utilization efficiency, i.e., the grain yield produced by unit weight of total accumulated K^+ per plant. St+L.S., Stem and leaf sheath; L.B., Leaf blade; B.R., Brown rice; R.H., Rice hull. Detailed data of other agronomic traits are provided in Supplemental Figure S5. The box plots and t-tests are as in Figure 2. Significant differences from the corresponding WT are indicated by asterisks (*, $P<0.05$; **, $P<0.01$; ***, $P<0.001$).

Figure 7. Effect of *OsHAK18* expression level on K^+ and Na^+ transport and distribution in rice supplied with NaCl in the culture solution.

Ten-day-old seedlings were grown in IRRI solution containing 1 mM K^+ for 4 weeks, then transferred to a solution containing additionally 20 mM NaCl and allowed to grow for 3 d. A-D, The phloem sap was collected and analyzed. E-L, After 20 mM NaCl treatment for 3 d, seedlings were transferred to IRRI solution without NaCl for 3 days. K^+ or Na^+ fraction (%) represents the percentage of K^+ or Na^+ content in each plant part to the total K^+ or Na^+ content of the whole plant. L.S., Leaf sheath; L.B., Leaf blade. The box plots and t-tests are as in Figure 2. Significant differences from the corresponding WT are indicated by asterisks (*, $P<0.05$; **, $P<0.01$; ***, $P<0.001$).

Figure 8. A working model for the roles of OsHAK18 in K^+ redistribution in the leaf blades and nodes of rice.

A, The role of OsHAK18 in the short distance transport of K^+ in a source leaf. B, The role of OsHAK18 in a node. CC, companion cell; DVB, diffuse vascular bundle; EVB, enlarged vascular bundle; MC, mesophyll cell; MS, mestome sheath cell; PPC, phloem parenchyma cell; VBS, vascular bundle sheath cell; XPC, xylem parenchyma cell. The size of arrows in the phloem and xylem represents flow area.

REFERENCES

Ai PH, Sun SB, Zhao JN, Fan XR, Xin WJ, Guo Q, Yu L, Shen QR, Wu P, Miller AJ, Xu GH (2009) Two rice phosphate transporters, OsPht1;2 and OsPht1;6, have different functions and kinetic properties in uptake and translocation. The Plant Journal 57: 798-809

Anschutz U, Becker D, Shabala S (2014) Going beyond nutrition: regulation of potassium homoeostasis as a common denominator of plant adaptive responses to environment. Journal of Plant Physiology 171: 670-687

Ayre BG (2011) Membrane-transport systems for sucrose in relation to whole-plant carbon partitioning. Molecular Plant 4(3): 377-394

Babst BA, Braun DM, Karve AA, Baker RF, Tran TM, Kenny DJ, Rohlhill J, Knoblauch J, Knoblauch M, Lohaus G, Tappero R, Scherzer S, Hedrich R, Jensen KH (2022) Sugar loading is not required for phloem sap flow in maize plants. Nature Plants 8: 171-180

Cakmak I, Hengeler C, Marschner H (1994) Changes in phloem export of sucrose in leaves in response to phosphorus, potassium and magnesium deficiency in bean plants. Journal of Experimental Botany 45(9): 1251-1257

Cai J, Chen L, Qu HY, Lian J, Liu W, Hu YB, Xu GH (2012) Alteration of nutrient allocation and transporter genes expression in rice under N, P, K, and Mg deficiencies. Acta Physiologiae Plantarum 34: 939-946

Chang MX, Gu M, Xia YW, Dai XL, Dai CR, Zhang J, Wang SC, Qu HY, Yamaji N, Ma JF, Xu GH (2019) OsPHT1;3 mediates uptake, translocation, and remobilization of phosphate under extremely low phosphate regimes. Plant Physiology 179: 656-670

Chen G, Hu QD, Luo L, Yang TY, Zhang S, Hu YB, Yu L, Xu GH (2015) Rice potassium transporter OsHAK1 is essential for maintaining potassium-mediated growth and functions in salt tolerance over low and high potassium concentration ranges. Plant, Cell & Environment 38(12):2747-2765

Crafts AS, Crisp CE (1972) Phloem transport in plants. Bioscience 22(1): 56-57

Dai CR, Dai XL, Qu HY, Men Q, Liu JY, Yu L, Gu M, Xu GH (2022) The rice phosphate transporter OsPHT1;7 plays a dual role in phosphorus redistribution and anther development. Plant Physiology 188(4): 2272-2288

Deeken D, Geiger D, Fromm J, Koroleva O, Ache P, Langenfeld-Heyser R, Sauer N, May ST, Hedrich R (2002) Loss of the AKT2/3 potassium channel affects sugar loading into the phloem of Arabidopsis. Planta 216: 334-344

De Schepper V, De Swaef T, Bauweraerts I, Steppe K (2013) Phloem transport: a review of mechanisms and controls. Journal of Experimental Botany 64(16): 4839-50

Dreyer I, Gomez-Porras JL, Riedelsberger J (2017) The potassium battery: a mobile energy source for transport processes in plant vascular tissues. New Phytologist 216(4): 1049-1053

856 Epstein E, Rains DW, Elzam OE (1963) Resolution of dual mechanisms of potassium absorption by
857 barley roots. Proceedings of the National Academy of Sciences of the United States of America
858 49: 684-692
859 Feng HM, Tang Q, Cai J, Xu BC, Xu GH, Yu L (2019) Rice OsHAK16 functions in potassium uptake
860 and translocation in shoot, maintaining potassium homeostasis and salt tolerance. Planta 250 (2):
861 549-561
862 Gajdanowicz P, Michard E, Sandmann M, Rocha M, Corrêa LGG, Ramírez-Aguilar SJ, Gomez-Porras
863 JL, González W, Thibaud JB, van Dongen JT, Dreyer I (2010) Potassium (K^+) gradients serve as
864 a mobile energy source in plant vascular tissues. Proceedings of the National Academy of
865 Sciences of the United States of America 108(2): 864-869
866 Gaymard F, Pilot G, Lacombe B, Bouchez D, Bruneau D, Boucherez J, Michaux-Ferriere N, Thibaud
867 JB, Sentenac H (1998) Identification and disruption of a plant shaker-like outward channel
868 involved in K^+ release into the xylem sap. Cell 94: 647-655
869 Han M, Wu W, Wu WH, Wang Y (2016) Potassium transporter KUP7 is involved in K^+ acquisition and
870 translocation in Arabidopsis root under K^+-limited conditions. Molecular plant 9(3): 437-446
871 Hu W, Loka DA, Fitzsimons TR, Zhou Z, Oosterhuis DM (2018) Potassium deficiency limits
872 reproductive success by altering carbohydrate and protein balances in cotton (*Gossypium*
873 *hirsutum* L.). Environmental and Experimental Botany 145: 87-94
874 Huang YN, Yang SY, Li JL, Wang SF, Wang JJ, Hao DL, Su YH (2021) The rectification control and
875 physiological relevance of potassium channel OsAKT2. Plant Physiology 187: 2296-2310
876 Jia HF, Ren HY, Gu M, Zhao JN, Sun SB, Zhang X, Chen JY, Wu P, Xu GH (2011) The phosphate
877 transporter gene *OsPht1;8* is involved in phosphate homeostasis in rice. Plant Physiology 156:
878 1164-1174
879 Julius BT, Leach KA, Tran TM, Mertz RA, Braun DM (2017) Sugar transporters in plants: new insights
880 and discoveries. Plant and Cell Physiology 1: 1-55
881 Kim HY, Choi EH, Min MK, Hwang H, Moon SJ, Yoon I, Byun MO, Kim BG (2015) Differential gene
882 expression of two outward-rectifying shaker-like potassium channels OsSKOR and OsGORK in
883 rice. Journal of Plant Biology 58: 230-235
884 King RW, Zeevaart JAD (1974) Enhancement of phloem exudation from cut petioles by chelating
885 agents. Plant Physiology 53: 96-10
886 Knoblauch M, Peters WS (2016) Think outside the sieve element. Plant, Cell & Environment 39: 707-
887 708
888 Lalonde S, Tegeder M, Holst MT, Frommer WB, Patrick JW (2003) Phloem loading and unloading of
889 sugars and amino acids. Plant, Cell & Environment 26: 37-56
890 Leyva A, Quintana A, Sánchez M, Rodríguez E N, Cremata J, Sánchez J C (2008) Rapid and sensitive
891 anthrone–sulfuric acid assay in microplate format to quantify carbohydrate in biopharmaceutical

892 products: method development and validation. Biologicals, 36 (2) :134-141
893 Li WH, Xu GH, Alli A, Yu L (2018) Plant HAK/KUP/KT K^+ transporters: function and regulation.
894 Seminars in Cell & Developmental Biology 74: 133-141
895 Lu YX, Li CJ, Zhang FS (2005) Transpiration, potassium uptake and flow in tobacco as affected by
896 nitrogen forms and nutrient levels. Annals of Botany-London 95(6): 991-998
897 Lu GW, Coneva V, Rothstein SJ (2015) OsPIN5b modulates rice (Oryza sativa) plant architecture and
898 yield by changing auxin homeostasis, transport and distribution. The Plant Journal 83: 913-925
899 Luo L, Zhang YL, Xu GH (2020) How does nitrogen shape plant architecture? Journal of Experimental
900 Botany 71(15): 4415-4427
901 Maathuis FJM, Sanders D (1997) Regulation of K^+ absorption in plant root cells by external K^+:
902 interplay of different plasma membrane K^+ transporters. Journal of Experimental Botany 48: 451-
903 458
904 Maathuis FJM, Amtmann A (1999) K^+ nutrition and Na^+ toxicity: the basis of cellular K^+/ Na^+ ratios.
905 Annals of Botany-London 84: 123-133
906 Marschner H, Kirkby EA, Cakmak I (1996) Effect of mineral nutritional status on shoot-root partitioning
907 of photo assimilates and cycling of mineral nutrients. Journal of Experimental Botany 47: 1255-
908 1263
909 Michard E, Lacombe B, Porée F, Mueller-Roeber B, Sentenac H, Thibaud JB, Dreyer I (2005) A unique
910 voltage sensor sensitizes the potassium channel AKT2 to phosphoregulation. Journal of General
911 Physiology 126(6): 605-617
912 Munns R, Tester M (2008) Mechanisms of salinity tolerance. Annual Review of Plant Biology 59: 651-
913 681
914 Nieves-Cordones M, Martínez-Cordero M, Martínez V, Rubio F (2007) An $NH4^+$-sensitive component
915 dominates high-affinity K^+ uptake in tomato plants. Plant Science 172: 273-280
916 Pate JS, Jeschke WD (1995) Role of stems in transport, storage, and circulation of ions and
917 metabolites by the whole plant. Plant Stems 8:177-204
918 Peuke AD and Rennenberg H. (2011) Impacts of drought on mineral macro- and microelements in
919 provenances of beech (*Fagus sylvatica* L.) seedlings. Tree Physiology 31(2): 196-207
920 Philippar K, Buchsenschutz K, Abshagen M, Fuchs I, Geiger D, Lacombe B, Hedrich R (2003) The K^+
921 channel KZM1 mediates potassium uptake into the phloem and guard cells of the C_4 grass *Zea*
922 *mays*. The Journal of Biological Chemistry 278(19): 16973-16981
923 Prado FE, Boero C, Gallardo M, Gonzalez JA (2000) Effect of NaCl on germination, growth, and
924 soluble sugar content in *Chenopodium quinoa* Willd. Seeds. Botanical Bulletin of Academia Sinica
925 41: 27-34
926 Quintero FJ, Garciadeblás B, Rodríguez-Navarro A (1996) The SAL1 gene of Arabidopsis, encoding
927 an enzyme with 3′ (2′),5′-bisphosphate nucleotidase and inositol polyphosphate 1-phosphatase

activities, increases salt tolerance in yeast. The Plant Cell 8: 529-537

Ren ZH, Gao JP, Li LG, Cai XL, Huang W, Chao DY, Zhu MZ, Wang ZY, Luan S, Lin HX (2005) A rice quantitative trait locus for salt tolerance encodes a sodium transporter. Nature Genetics 37: 1141-1146

Roberts SK, Tester M (1995) Inward and outward K^+-selective currents in the plasma membrane of protoplasts from maize root cortex and stele. The Plant Journal 8: 811-825

Robert Turgeon (2010) The Puzzle of Phloem Pressure. Plant Physiology 154: 578-581

Ródenas R, García-Legaz MF, López-Gómez E, Martínez V, Rubio F, Ángeles Botella M (2017) NO_3^-, PO_4^{3-} and SO_4^{2-} deprivation reduced LKT1-mediated low-affinity K^+ uptake and SKOR-mediated K^+ translocation in tomato and Arabidopsis plants. Physiologia Plantarum 160: 410-424

Romano LA, Hendrik M, Assmann SM (1998) Ca^{2+}-Permeable, Outwardly-rectifying K^+ channels in mesophyll cells of *Arabidopsis thaliana*. Plant and cell physiology 39: 1133-1144

Rubio F, Nieves-Cordones M, Alemán F, Martínez V (2008) Relative contribution of AtHAK5 and AtAKT1 to K^+ uptake in the high-affinity range of concentrations. Physiologia Plantarum 134: 598-608

Rubio F, Alemán F, Nieves-Cordones M, Martínez V (2010) Studies on Arabidopsis athak5, atakt1 double mutants disclose the range of concentrations at which AtHAK5, AtAKT1 and unknown systems mediate K^+ uptake. Physiologia Plantarum 139: 220-228

Shabala S, Cuin TA (2008) Potassium transport and plant salt tolerance. Physiologia Plantarum 133: 651-669

Shin R (2014) Strategies for improving potassium use efficiency in plants. Molecules and Cells 37(8): 575-584

Steinacher A, Leyser O, Clayton RH (2012) A computational model of auxin and pH dynamics in a single plant cell. Journal of Theoretical Biology 296: 84-94

Sze H, Chanroj S (2018) Plant endomembrane dynamics: studies of K^+/H^+ antiporters provide insights on the effects of pH and ion homeostasis. Plant Physiology 177: 875-895

Tang Z, Fan XR, Li Q, Feng HM, Miller AJ, Shen QR, Xu GH (2012) Knockdown of a rice stelar nitrate transporter alters long-distance translocation but not root influx. Plant Physiology 160: 2052–2063

Tian QX, Shen LK, Luan JX, Zhou ZZ, Guo DS, Shen Y, Jing W, Zhang BL, Zhang Q, Zhang WH (2021) Rice shaker potassium channel OsAKT2 positively regulates salt tolerance and grain yield by mediating K^+ redistribution. Plant, Cell & Environment 44(9): 2951-2965

Turgeon R, Ayre BG (2005) Pathways and mechanism of phloem loading. Vascular Transport in Plants 3: 45-67

Van Bel AJE (2003) The phloem, a miracle of ingenuity. Plant, Cell & Environment 26: 125-149

Wegner LH, Raschke K (1994) Ion channels in the xylem parenchyma of barley roots (a procedure to isolate protoplasts from this tissue and a patch-clamp exploration of salt passage ways into xylem

964 vessels. Plant Physiology 105: 799-813
965 White PJ, Ding GD (2022) Long-distance transport in the xylem and phloem. In: Marschner's Mineral
966 Nutrition of Higher Plants, the 4th edition, edited by Rengel Z, Cakmak I, White PJ. 3: 73-104.
967 Academic Press, London EC2Y5AS, United Kingdom.
968 Xie B, Hong ZL (2011) Unplugging the callose plug from sieve pores. Plant Signaling & Behavior 6(4):
969 491-493
970 Yamaji N, Ma JF (2007) Spatial distribution and temporal variation of the rice silicon transporter Lsi1.
971 Plant Physiology 143: 1306-1313
972 Yang TY, Zhang S, Hu YB, Wu FC, Hu QD, Chen G, Cai J, Wu T, Moran N, Yu L, Xu GH (2014) The
973 role of a potassium transporter OsHAK5 in potassium acquisition and transport from roots to
974 shoots in rice at low potassium supply levels. Plant Physiology 166: 945-959
975 Yang TY, Feng HM, Zhang S, Xiao HJ, Hu QD, Chen G, Xuan W, Moran N, Murphy A, Yu L, Xu GH
976 (2020) The Potassium Transporter OsHAK5 Alters Rice Architecture via ATP-Dependent
977 Transmembrane Auxin Fluxes. Plant Communications 1(5): 1-15
978 Yoshida S, Forno DA, Cock JH, Gomez KA (1976) Routine Procedures for Growing Rice Plants in
979 Culture Solution, Ed 3. International Rice Research Institute, Los Banos, Philippines